



*Sudan University of Science and
Technology*

*Collage of Petroleum Engineering and
Technology*



Exploration Engineering Department

Evaluation For Aradieba Formation In Bamboo Field

تقييم طبقة عرديبه في حقل بامبو

*Project submitted in partial fulfillment of requirement of the degree of
B.sc In petroleum engineering*

Prepared by:

1. Ahmed Ali Said Ahmed.
2. Hassab Alrasool Emad Noor Aldaim.
3. Mohammed Aljiely fadol allah.
4. Mohammed Yousif Hassan Alfaki.

Supervisor:

Dr. Ahmed ABdalaziz Ibrahim

September 2014

Evaluation For Aradieba Formation In Bamboo Field

تقييم طبقة عرديبه في حقل بامبو

مشروع تخرج مقدم الي كلية هندسة وتكنولوجيا النفط - قسم الاستكشاف - جامعة السودان للعلوم والتكنولوجيا

انجاز جزئي لاحد المتطلبات للحصول علي درجة البكالوريوس في الهندسة

اعداد الطلاب :

1- احمد علي سيد احمد.

2- حسب الرسول عماد نور الدائم.

3- محمد الجيلي فضل الله.

4- محمد يوسف حسن الفكي.

تمت الموافقة علي هذا المشروع من كلية هندسة وتكنولوجيا النفط الي قسم هندسة النفط

التوقيع.....

المشرف علي المشروع: د.م. احمد عبد العزيز ابراهيم

التوقيع.....

رئيس قسم هندسة النفط: ا.م. فاطمة احمد التجاني

التوقيع.....

عميد كلية هندسة وتكنولوجيا النفط: د.م. سمية عبد المنعم

التوقيع.....

التاريخ: 2014/ 9 /

الاستهلال

بسم الله الرحمن الرحيم

قال تعالى :

(الله لا اله الا هو الحي القيوم لا تأخذه سنة ولا نوم له ما في
السموات وما في الأرض من ذا الذي يشفع عنده إلا
بإذنه يعلم ما بين أيديهم وما خلفهم ولا يحيطون بشي
من علمه إلا بما شاء وسع كرسيه السموات والأرض ولا يؤدوه
حفظهما وهو العلي العظيم) . صدق الله العظيم.

الإهداء

يا جنتي في الدنيا والآخرة .. يا حبيبتي وكل كياني .. تظلين لي رمز الطهارة والنقاء .. منارة الحب والحنان ..
سلسبيل الوفاء الأبدى .. نهر العطاء المتجدد... الذي لا ينضب ..

يا من أروضعتني الحب والحنان

يا رمز الحب وبلسم الشفاء

إلى القلب الناصع بالبياض (والدتي الحبيبة) ...

إلى من جرع الكأس فارغا ليسقني قطرة حب

إلى من كنت أنامله ليقدم لنا لحظه سعادة

إلى من حصد الأشواك عن دربي ليمهد لي طريق العلم

إلى القلب الكبير (والدي العزيز) ...

إلى القلوب الطاهرة الرقيقة والنفوس البريئة إلى رياحين حياتي (إخوتي)

الآن تفتح الأشرعة وترفع المرساة لتتطلق السفينة في عرض بحر واسع مظلم هو بحر الحياة وفي هذه الظلمة
لا يضيء إلا قنديل الذكرى ذكرى الإخوة البعيدة إلي الذين أحببناهم وأحبونا في الله سبحانه وتعالى ()
أصدقائي .

كلمة شكر و عرفان

لأبد لنا ونحن نخطو خطواتنا الأخيرة في الحياة الجامعية من وقفة نعود إلي أعوام قضيناها في رحاب الجامعة
مع أساتذتنا الكرام الذين قدموا لنا الكثير باذلين بذالك جهودا كبيرة في بناء جيل الغد لتبعث الأمة من

جديد ... وقبول أن نمضي. نقدم أسمى آيات الشكر والعرفان والامتنان والتقدير والمحبة إلي الذين حملوا
أقدس رسالة في الحياة ...

إلي الذين مهدوا لنا طريق العلم والمعرفة

إلي جميع أساتذتنا الأفاضل .

"كن ... عالما فإن لم تستطيع فكن متعلما فإن لم تستطيع فأحب العلماء فإن لم تستطع فلا تبغضهم "

ونخص بالشكر والتقدير:

الدكتور : احمد عبد العزيز إبراهيم

الدكتورة : تقوي احمد موسى

الأستاذ: عمرو يوسف

الأستاذ : محمد عبد الخالق

المهندس: عمار

المهندس: رامي سليم

الذين نقول لهم بشراكم قول رسول الله صلى الله عليه وسلم :

"إن الحوض في البحر ، والطير في السماء، ليصلون علي معلم الناس الخير "

كما إننا نتوجه له بخالص الشكر والعرفان

الدكتور احمد عبد العزيز إبراهيم (شكرا معلمنا العزيز)

وكذلك نشكر كل من ساعد على إتمام هذا البحث وقدم لنا العون ومد لنا يد المساعدة وزودنا بالمعلومات اللازمة
لإتمامه.

list of Figures

NO	TITLE	Page
1-1	Geological map of Sudan	3

1-2	Map of Muglad basins	4
1-3	Greater Bamboo area Map	6
1-4	The Structure Map of Bamboo West Field	7
2-1	Different type of porosity	11
2-2	Poroperm cross-plot for clean sandstone and a carbonate	20
2-3	Poroperm Relationships	21
2-4	Poroperm cross- plot and the influence of grain size	22
3-1	Shale interval travel time VS depth	26
3-2	Algorithmic plot of shale resistivity VS linear depth	28
3-3	Response of shale acoustic transit time to abnormal pressure	28
4-1	Map explain the effective porosity distribution for Arabeiba formation in bamboo field	41
4-2	Porosity Versus Permeability from Coring data	42
4-3	Explain the permeability distribution for Arabeiba formation in bamboo field	45
4-4	Explain the saturation distribution by Archi equation for Arabeiba formation in bamboo field	49
4-5	Sonic vs Density	51
4-6	Sonic vs Depth	51
4-7	Pressure calculated Versus Depth	52
4-8	Explain the pressure estimated distribution for Arabeiba formation using Sonic equation	53
5-1	Saturation contour map	56
5-2	Effective porosity contour map	56
5-3	Permeability contour map	57
5-4	Pressure contour map	57
5-5	Plot pressure VS Depth	58
5-6	Plot saturation by Archi equation and by Indonesian(IP) VS Depth	58
5-7	Plot calculated permeability and permeability by IP VS Depth	59
5-8	Plot calculated porosity and porosity by IP VS Depth	59
5-9	Locations with good probability	60

List of Table

NO	TITLE	
----	-------	--

		PAGE
1-1	The lithology and environments of Muglad basins	5
2-1	The Range Of porosity Values For rocks	11
2-2	Reservoir permeability classification	17
2-3	Empirical approximations for calculating permeability	19
4-1	Log data required for well 1	33
4-2	Log data required for well 3	33
4-3	Log data required for well 4	34
4-4	Log data required for well 6	34
4-5	Log data required for well 7	35
4-6	Total porosity for well 1	36
4-7	Total porosity for well 3	36
4-8	Total porosity for well 4	37
4-9	Total porosity for well 6	37
4-10	Total porosity for well 7	38
4-11	Effective porosity for well 1	39
4-12	Effective porosity for well 3	39
4-13	Effective porosity for well 4	40
4-14	Effective porosity for well 6	40
4-15	Effective porosity for well 7	41
4-16	Permeability for well 1	43
4-17	Permeability for well 3	43
4-18	Permeability for well 4	44
4-19	Permeability for well 6	44
4-20	Permeability for well 7	45
4-21	Saturation for well 1	46
4-22	Saturation for well 3	47
4-23	Saturation for well 4	47
4-24	Saturation for well 6	48
4-25	Saturation for well 7	48

التجريد

يهدف هذا البحث إلى تقييم طبقة عرديية في حقل بامبو , عن طريق حساب عدد من الخصائص الفيزيائية للطبقة (المسامية والنفاذية، والتشبع والضغط). تم حساب هذه الخصائص بناء على بيانات تسجيلات

الإبار وذلك للحصول على خرائط كنتورية تبين توزيع هذه الخصائص للطبقة في الحقل من خلال خمسة آبار تم اختيارها لتكون موضع الدراسة. من نتائج هذه الدراسة يسهل اتخاذ القرارات اعتمادا على كمية من المواد الهيدروكربونية في الطبقة والتي يستدل عليها من خلال الخصائص المحسوبة وبالتالي معرفة الجدوى الاقتصادية من هذا الحقل.

Abstract

This research aims to evaluate the Aradeiba formation of bamboo field of .by calculating the number of physical properties of formation (porosity, permeability, saturation and pressure)

These properties have been calculated based on log data so as to get the contour maps showing the distribution of these properties in the field through five wells have been selected to be the case of study.

Results of this study, facilitates decision-making depending on the amount of hydrocarbons in the field and inferred through the properties calculated and therefore know the economic feasibility of the field.

Content

الاستهلال.....	III
الإهداء	III
كلمة شكر و عرفان	IV
FIGURES LIST OF.....	V
LIST OF TABLE.....	VI
التجريد	VII
ABSTRACT	IX
INTROUCTION	- 1 -
1.1. SUDAN GEOLOGICAL:	- 3 -
1.2. MUGLAD BASIN:	- 4 -
1.2.1. Tectono-Stratigraphic Development of Muglad Basin	- 6 -
1.3. GREATER BAMBOO	- 9 -
1.3.1. Structure map and well profile:	- 10 -
1.4. Aradeiba Formation:.....	- 11 -
1.4.1. Lateral Seal:.....	- 12 -
CHAPTER 2	- 20 -
2.1. POROSITY	- 20 -
2.1.1. Introduction:.....	- 20 -
2.1.2. Porosity Types:.....	- 21 -
2.1.3. The Range of Porosity Values in Nature:.....	- 22 -
2.1.4. Porosity Logs:	- 23 -
2.1.5. Total Porosity Determination:	- 25 -
2.1.6. Calculating The Porosity:.....	- 25 -
2.1.7. Porosity by Coring:.....	- 25 -
2.2. PERMEABILITY.....	- 26 -
2.2.1. Definition and theory:.....	- 26 -
2.2.2. Controls on Permeability and the Range of Permeability Values.....	- 28 -
2.2.3. Permeability Determination:	- 29 -
2.2.4. Type of Permeability:	- 29 -
2.2.5. Permeability Relationships:	- 30 -
CHAPTER 3	- 35 -
3.1. HYDROSTATIC PRESSURE:	- 35 -
3.2. OVERBURDEN PRESSURE:	- 36 -
3.3. PORE PRESSURE:	- 36 -
3.3.1. Normal Pore Pressure:	- 36 -
3.3.2. Abnormal Pore Pressure:.....	- 37 -
3.3.3. Subnormal Pore Pressure:	- 37 -
3.4. PORE PRESSURE EVALUATION:	- 37 -

3.4.1. Sonic Logs:.....	- 37 -
3.4.2. Resistivity Logs:	- 39 -
3.4.3. Formation Density Logs:.....	- 40 -
3.5. SATURATION:	- 40 -
3.5.1. Mathematical expressions for fluid saturation:.....	- 41 -
3.5.2. Methods to Determination Saturation:.....	- 42 -
CHAPTER 4	- 44 -
4.1. POROSITY CALCULATION	- 44 -
4.1.1. Total porosity:	- 44 -
4.1.2. Effective Porosity:	- 50 -
4.2. PERMEABILITY.....	- 54 -
4.3. SATURATION:	- 58 -
4.4. PORE PRESSURE.....	- 61 -
4.4.1. Numerical Methodology for Pressure Estimation:	- 61 -
4.4.2. Pressure Numerical Estimation:.....	- 62 -
4.4.3. Pore pressure Estimation Method:	- 62 -
CHAPTER 5	- 67 -
RESULT AND DISCUSION	- 67 -
CONCLUSION AND RECOMMENDATION	- 74 -
CONCLUSION :	- 74 -
RECOMMENDATION:.....	- 75 -
REFERENCES :	- 76 -
APPENDIX	- 78 -

INTROUCTION

This study focused in evaluate Aradieba layer of Bamboo field west through the distribution of following properties: porosity, permeability, pressure and saturation in the field by using contours maps.

Formation evaluation in the oil industry is very important because it is based on many operation such as establish reservoir and OOPI and whether or not economic oil quantity . It also helps to know optimum well location and the depth of layer containing the oil thus where the perforation. In addition, utilized to avoid some problem like blow out.

The basic objective of the project was evaluated Aradieba layer in bamboo west to get porosity, permeability, pressure and saturation in the layer .

There are many problem and constraints encountered in the completion of the project, like the difficulty obtaining data of well logging (lass file), but was solved through calibration with some engineers. As we faced difficulty with software (IP) but processed this problem by consulting number of software professional in the petroleum industry. Also couldn't get chance to visit the field to obtain more information

After obtaining the data we used the number of equations and assumptions of the previous properties to achieve this end, we hired a number of software.

This research Serve the purposes exploration and development together, where it presents a study of the field based on specific wells data from the field, allowing the opportunity to know zones in the field that are not available them data as the data is available in the zones wells only be in the form of a vertical in the direction of the well while when generalize these properties on the entire field, it helps to know what the gradient of these properties at the field level and thus serves the purposes exploratory in terms of knowledge of places that can contain these properties calculated (porosity, permeability, saturation and pressure) very well and places that have these properties from this are inferior results obtained it builds on the basis of the methods used to develop the field and increase the productivity of it.

Chapter 1

Geological Background

1.1. Sudan geological:

Sudan geological study was focused on the surface geology mainly for surface mapping and limited shallow mining activities.

With the recent discovery of commercial hydrocarbon, extensive subsurface data has been acquired both offshore and onshore.

These data revealed existence of several sedimentary basins offshore in the Red Sea and onshore in the interior Sudan, the Main sedimentary Basins are shown in Geological map of Sudan in Figure (1-1).

These basins are all rift basins, owing their existence to the rifting activities of Western, Central and East African Rift Systems.

Exploration is still at early stages and the data collected is scarce. based on the available data and from analogy to other basins it can be concluded that the major conditions for Petroleum accumulations have been met.

Hundreds of meters of rich source rocks have been penetrated in Muglad, Melut, Blue Nile, Red Sea, Khartoum, and White Nile Basins.(Oil Opportunities in Sudan,2013).

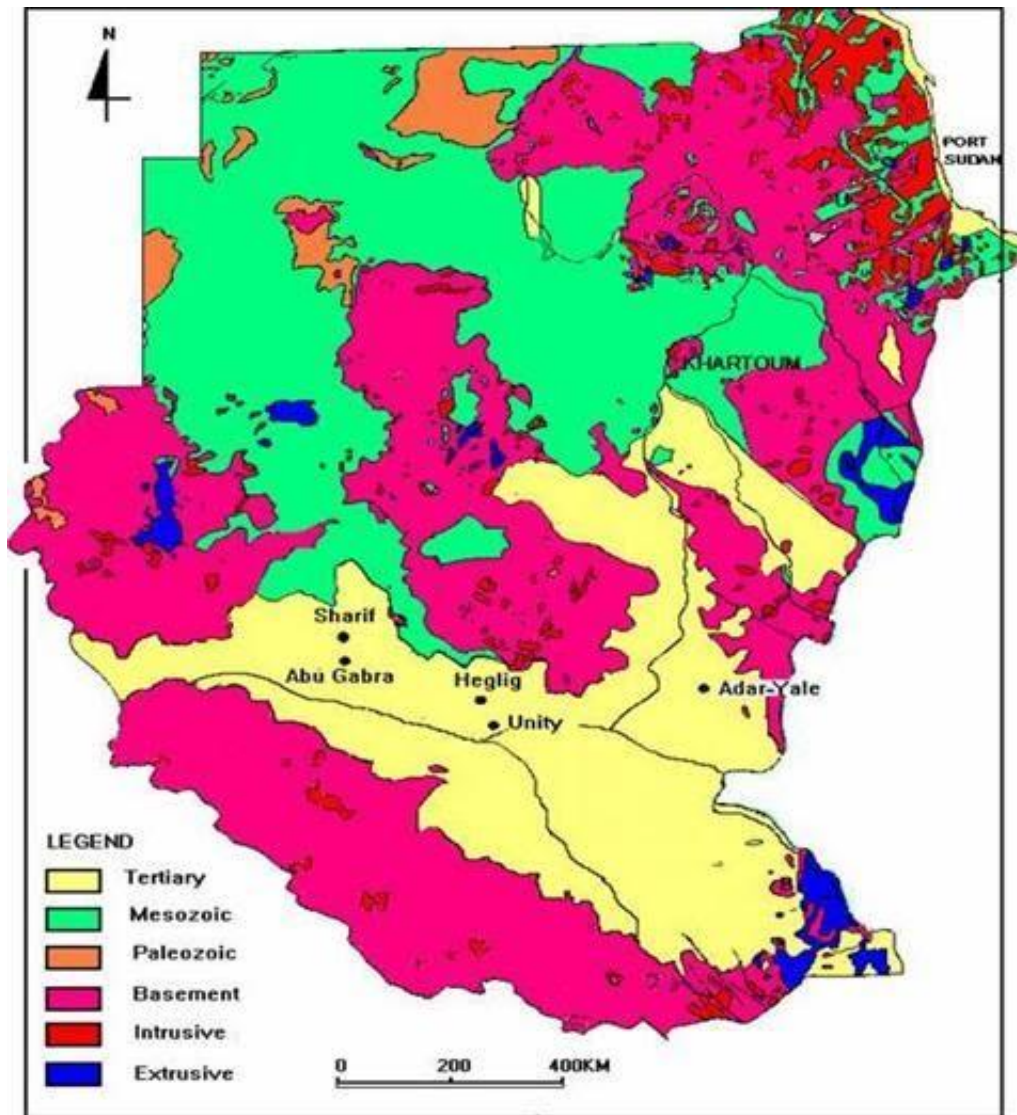


Figure (1-1) Geological map of Sudan (Oil opportunities in Sudan,2013)

1.2. Muglad Basin:

The Muglad basin is rift basin of Meso-cenozoic, which caused by the shear zone of middle-Africa and developed on the firm basement of Precambrian(Vail,1978; Whiteman, 1971). There are three superimposed rift formations of different periods in Muglad area since Early Cretaceous(Fairhead, 1988). The first one is Abu Gabra Fm - Bentiu Fm of Lower Cretaceous, the second one is the Darfour group of Upper Cretaceous–Paleocene of Paleogene, and the third is Eocene of paleogene–Neogene. There are immense differences in the position of main extensional faults of the three rifts, the early rift was cut and changed by the later rift (Fairhead, 1988).

The major rift formation in discoveries Abu Gabra and Sharif belong to the first and

second periods, deposition formation of the third period is very poor. The rift sign of main extensional fault system of the first period is indistinct for the reason of datum. The generation of second period rift resulted mostly from the action of dextral slip of share zone of middle-Africa, the direction of main faults in work area is NW. Though the deposition of third period rift in work area is thin, it changed the early rift obviously. The third period rift was under the control of series action of East African Rift Valley (Schull 1988; Kaska 1989).

The initiation of rifting in southern Sudan might be directly related to Jurassic rifting in northern Kenya (Anza Trough) or to the older Karoo rifts known in Eastern Kenya and Madagascar. Possible evidence for the timing of the rift initiation is the Jurassic sedimentary sequence encountered in the Blue Nile well or older sediments encountered in the deep Muglad and Melut basins (Schull,1988).

The second rifting phase began during the Coniacian-Santonian times and continued until the end of Cretaceous(Schull 1988).

Changes in the opening of the South Atlantic account for a Late Cretaceous period of shear movements on the West and Central African rift system (Santonian shear in the Benoue trough) (Fairhead ,1988).

The third rifting phase is recorded in a thick accumulation of over 3960 m of sediments. The intensely faulted section of the Early Tertiary of the southern Sudan basins indicates that this final rifting phase was a significant tectonic event(Lowell & Genik 1972).

The initiation of this rifting phase is synchronous to the initial phase of the opening of the Red Sea and East African rifting: the Muglad, Melut, and Blue Nile basins are sub-parallel to the Red Sea(Schull,1988).the following figure (1-2) show a map of muglad basins.

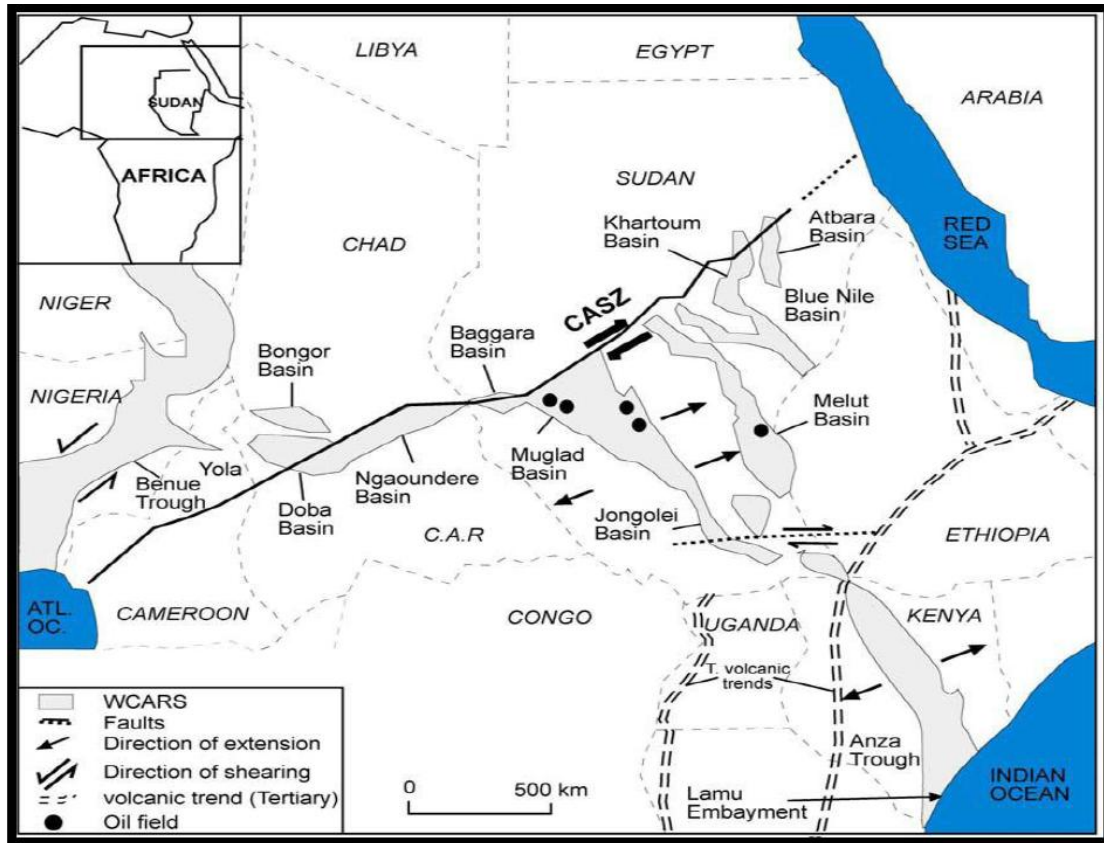


Figure (1-2) map of Muglad basins (GNPOC, 2009)

1.2.1. Tectono-Stratigraphic Development of Muglad Basin

The tectonic development of this area can be divided into a pre-rift phase and three rift phases, while each rift phase is followed by a sag phase. These evolutionary stages are well documented by geophysical data, well information, and regional geology (Schull,1988).

The basement adjacent to the Muglad basin is predominantly Precambrian and Cambrian metamorphic rocks with limited occurrences rock of intrusive igneous.

The following table (1-1) show the Lithology and Environments of Muglad basins.

1.2.1.1. Pre-Rifting Phase:

By the end of the Pan-African orogenesis (550 ±100 Ma), the region became a consolidated platform. During the Paleozoic and Early Mesozoic, this highland platform provided the sediments for the adjacent subsiding areas. The nearest preserved Paleozoic rocks are continental sediments in northwest Sudan, close to the Chad and Libyan borders. (Schull,1988).

1.2.1.2. Rifting phases:

As mentioned above, three distinct periods of rifting occurred in response to crustal extension, which provided the isostatic mechanism for subsidence. Subsidence was accomplished by normal faulting parallel and sub-parallel to the basin axes and margins. The multiphase tectonic history of the Muglad rift includes three discrete major extension phases: an Early Cretaceous (145 to 93.5 Ma), a Late Cretaceous (93.5 to 58 Ma) and an Eocene-Oligocene (58 to 23.8 Ma) rift phase, resulted in an accumulation of up to 5400m, 4200m and 5400m of sediments, respectively. Each phase consists of a rift-initiation phase, an active rifting phase and a thermal sag phase (Browne and Fairhead 1983; Schull, 1988).

1.2.1.2.1. The Initial Rifting Phase :

Cannot be dated precisely. In the case where the basement was penetrated by wells in the north-western Muglad basin, it is overlain by Neocomian- Barremian lacustrine siltstones and claystones attributed to Abu Gabra Formation. Seismic shows that the Abu Gabra is not a monolithic formation, but has a basal member affected by half graben tectonic (Schull, 1988). This basal member rests unconformably below an upper member, which is usually conformable with the overlying Bentiu Formation. Based on well and seismic data, it is suggested that the rifting begun during the Jurassic or Early Cretaceous (160-130 Ma.) and lasted until the end of the Aptian. The termination of the initial rifting without volcanism in Sudan is Stratigraphically marked by basin wide deposition of the thick sandstones of the Bentiu Formation (Schull, 1988).

• **Bentiu Sag Phase:**

Up to 3500 m of sands attributed to Bentiu Formation were deposited during the first sag phase. The average thickness of the Upper Bentiu, present all over the graben, is about 2000m. Whereas two local thickenings in the North Kaikang and South Kaikang troughs at the base of the formation (Lower Bentiu) amount 1500 m (Browne et al., 1985).

1.2.1.2.2. The Second Rifting Phase:

Occurred during the Coniacian up to Campanian-Maastrichtian (Darfur Group, Baraka Formation). Stratigraphically, this phase is seen in a widespread deposition of lacustrine and floodplain claystones and siltstones (Aradeiba shaly Formation) with minor volcanism in the northwestern part of the Muglad basin and in the central Melut

Basin. The end of this phase is marked by the deposition of an increasingly sand-rich sequence that concluded with thick Paleocene sandstone deposition of the Amal Formation (sag phase)(Schull,1988).



1.2.1.2.3. The Final Rifting Phase:

Began in the Late Eocene-Oligocene. This phase is reflected in the sediments by a thick sequence of lacustrine and floodplain claystones and siltstones with minor volcanism in the southern Melut block. After this rift period deposition became more sand-rich throughout the Late Oligocene-Miocene (Schull, 1988).

- **Adok Upper Sag Phase:**

During the middle Miocene, the basinal areas entered into an intra-cratonic sag phase of very slow subsidence accompanied by small or no faulting. This phase is marked by the deposition of 3000 m of sandy sediments and locally minor volcanism. In the Late Tertiary, the regional stress regime changed resulting in the termination of the southern Sudan rifting during the middle Miocene. A maximum of 762 m sediment thickness accumulated in these basins during the post-rift sag phase, the direction of the faults in work area is NNW.

Table (1-1) The Lithology and Environments of Muglad Basin (Shams Elfalah, 2009)

FORMATION		LITHOLOGY AND ENVIRONMENTS	AGE	
K O R D O F A N	Zeraf Fm.	Predominantly iron-stained sands and silts with minor claystones interbeds.	Recent-middle Miocene	T E R T I A R Y
	Adik Fm.	Braided streams/alluvial fans.	Oligocene-	
	Tendi Fm.	Predominantly claystone/shale, interbedded with sandstones	Late Eocene	
	Nayil Fm.	Fluvial/floodplain & lacustrine		
	Amal Fm.	Predominantly massive medium to coarse sandstones sequences. Braided streams/alluvial fans.	Paleocene	
D A R F U R G R O U P	Baraka Fm.	Predominantly sandstones with minor shales and claystones interbeds.	Late Senonian Turonian	C R E T A C E O U S
	Ghazal Fm.	Fluvial/alluvial fans.		
	Zarga Fm.	Predominantly sandstones shales with interbeds of siltstones and sandstones.		
	Aradeiba Fm.	Floodplain/lacustrine with fluvial/deltaic channel sands.		
Bentiu Fm.		Predominantly thick sandstones sequences. Braided/meandering streams.	Cenomanian Late Albian	
Abu Gabra Fm.		Predominantly claystones and shales with fine sandstones and siltstones. Lacustrine/deltaic.	Albian-Aptian	
Sharaf Fm.		Claystones, shales with interbeds of fine sandstones and siltstones. Lacustrine/fluvial floodplain.	Barremian Neocomian	
 Source rocks  Reservoir rocks				

1.3. Greater Bamboo

Greater Bamboo area show in Figure (1-3) lies about 30 km north of Heglig field in block 2A of Muglad Basin in Southern part of Sudan and covers an area of about 120 Sq.Km. The area is divided into four producing fields namely Bamboo, Bamboo West, Bamboo South and Bamboo East (Ayah Abdelhai Fadlallah Hussein , 2012).

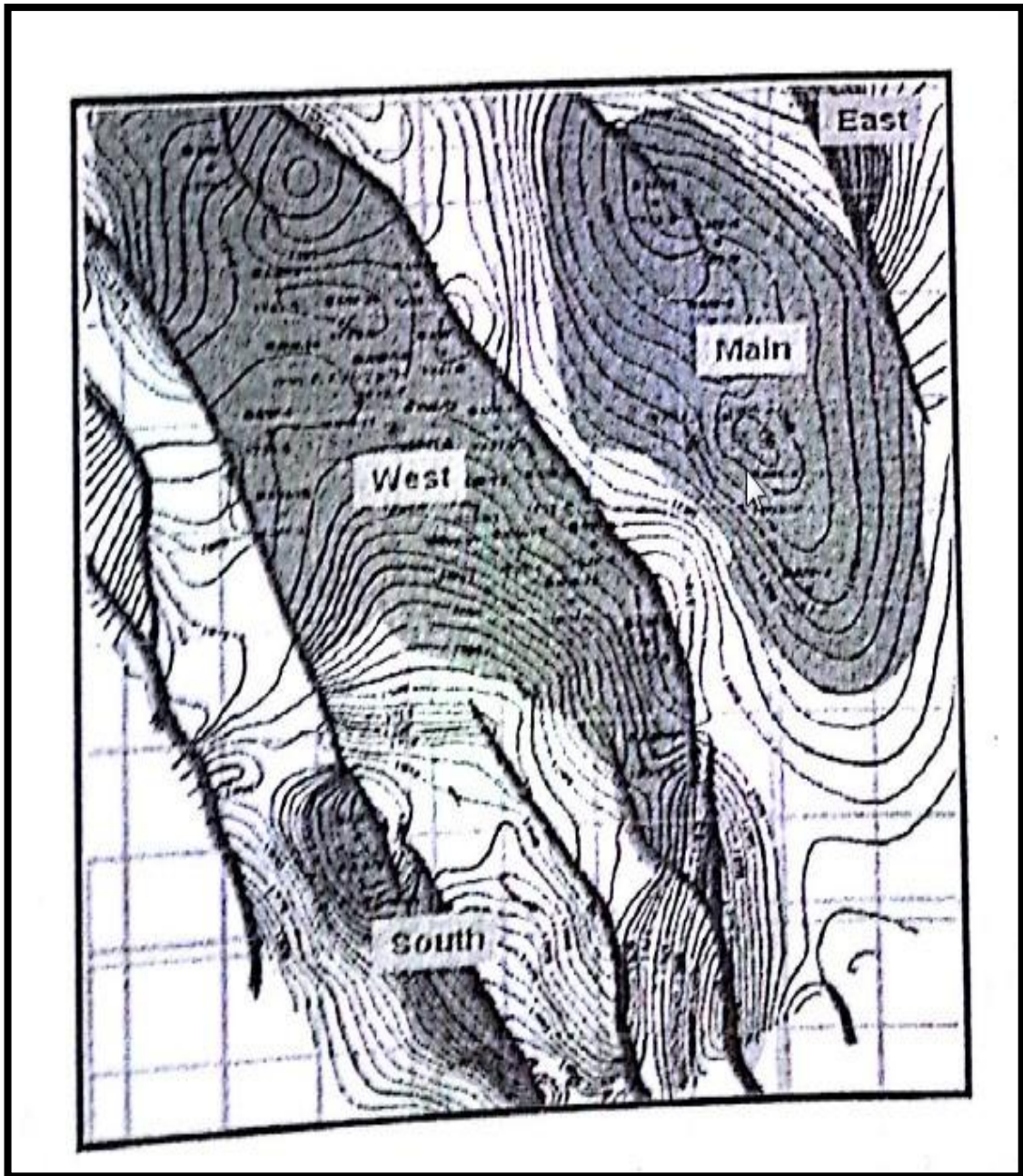


Figure (1-3) Greater Bamboo area map (GNPOC, 2009)

1.3.1. Structure map and well profile:

Bamboo west area was selected as the study area in this study choosing five wells are BAW-01, BAW-3, BAW-4, BAW-6, BAW-7 which are spread across the field in five different locations show in figure (1-4).

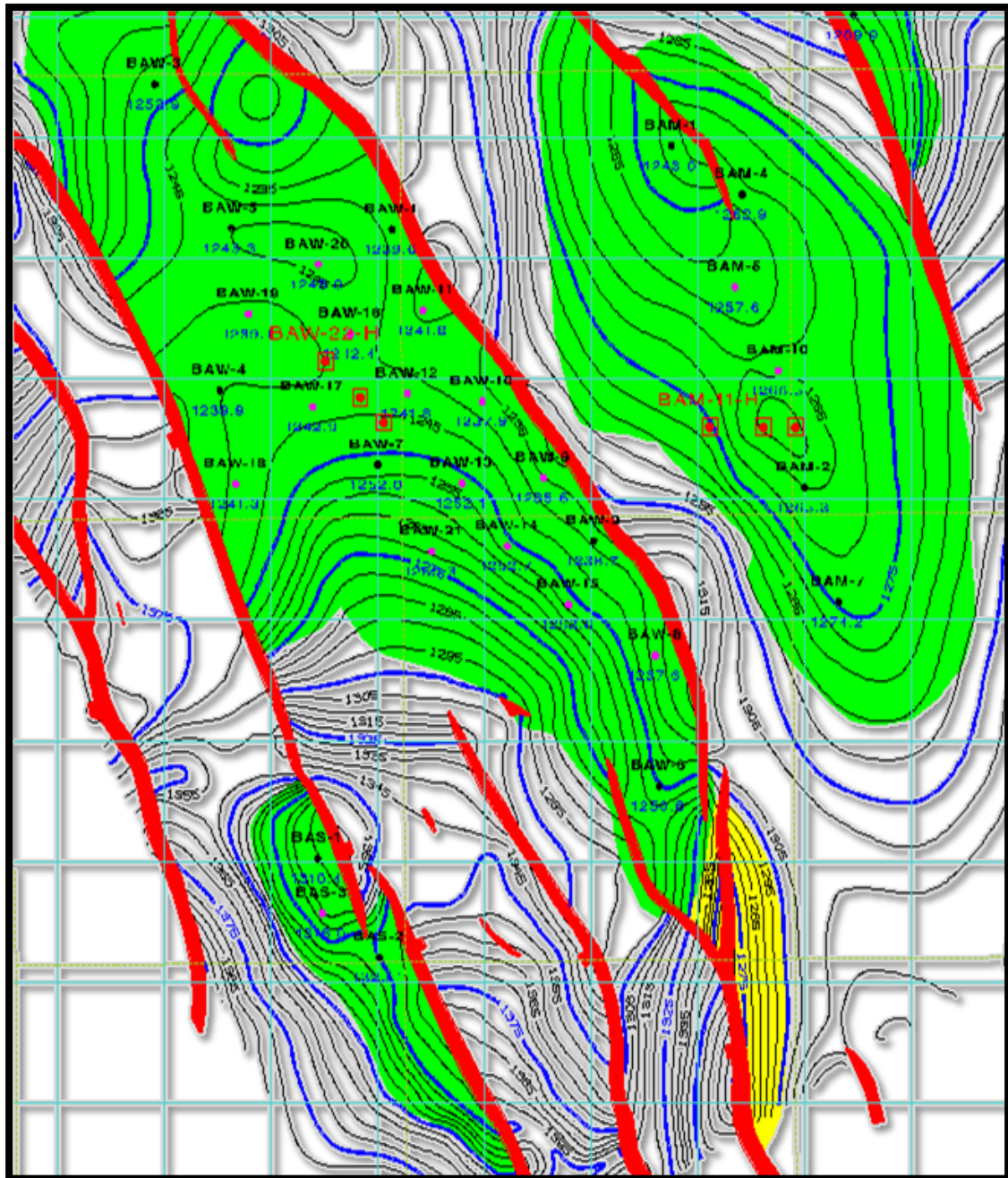


Figure (1-4) The Structure Map Of Bamboo West Field (GNPOC, 2009).

1.4. Aradeiba Formation:

The Aradeiba Formation consists of thick shale with inter-bedded lenses of sand stone. The top of Aradeiba Formation coincides with the onset of a peak which can be very well correlated over the entire area. Correlation of Aradeiba top was not undertaken since the reservoir sand Aradeiba-E is closer to Bentiu top than that of Aradeiba top, Aradeiba-E being the lowermost section of the Aradeiba Formation. In the model building process Aradeiba-E was projected from Bentiu top by adding isopach of Aradeiba-E to Bentiu top.

Aradeiba Formation sandstone is the main secondary reservoirs in the study area, with average thickness about 43 m. The Upper Cretaceous Darfur Group is predominantly composed of clay stones and thin interceded sandstone. The clay stone is reddish brown to dark brown and moderately hard. Sandstone from core description is light brown-grey color, massive to large trough cross-bedded. Core analysis of Aradeiba sand in Shelungo North_1 shows that the porosity of the Aradeiba E range from 21% to 27% averaged 26.2% (Mohammed, 2003). Generally Aradeiba sands are deposited in lower energy environment (Late Cretaceous (95-65 Ma)) with a much lower Rw. (RRI, 1991). (Shams Elfalah , 2009).

1.4.1.Lateral Seal:

Lateral seal depends on the thickness and the lithology of the Aradeiba shale and the amount of fault throw. Figure 4 is schematic illustration of this relationship. The Aradeiba Formation is highly variable in thickness and in sand/shale ratio. Thickest Aradeiba Formation penetration to date is in excess of 1000 m in the central part of the basin , decreasing to less than 20 m along the basin edges. Most of the perfect lateral seals are due to direct juxtaposition of Bentiu sandstone reservoirs against Aradeiba shale. Examples of this situation are illustrated in Figures. (1-5) to (1-11).

In some cases clay smear and shale gouge ratio play an important role in lateral seal integrity. The shale gouge ratio seems to depend on shale thickness and amount of displacement along the fault plane. Shale gouge will, of course, also depend on clay mineralogy, but this aspect has not been fully investigated. (Giedt, Norman, R., 1990)

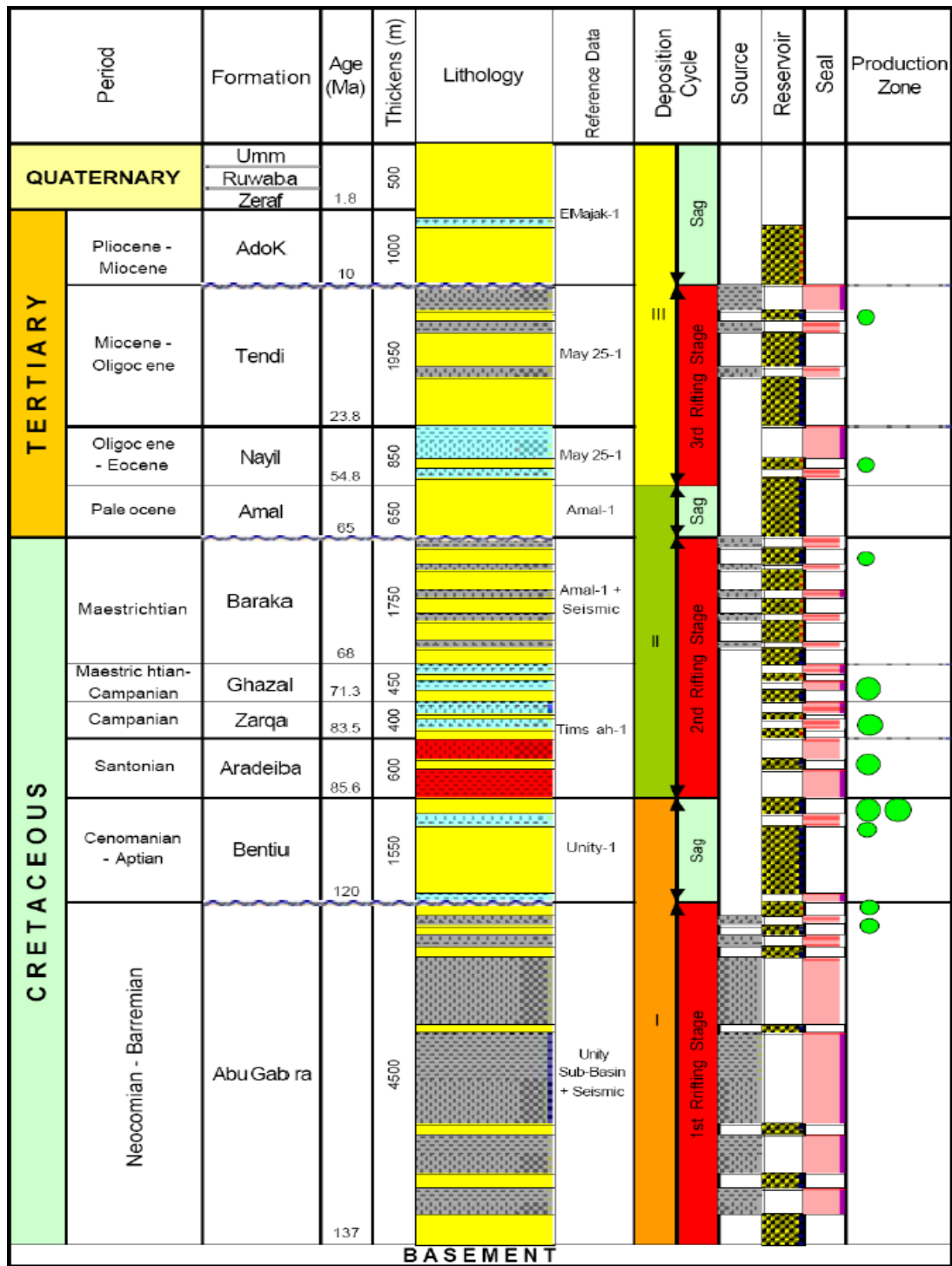


Figure (1-5). General stratigraphic column - Muglad Basin, Sudan, showing three geological cycles—Neocomian to Barremian, Aptian to Maestrichtian, and Paleocene to Pliocene/Miocene, or Quaternary.

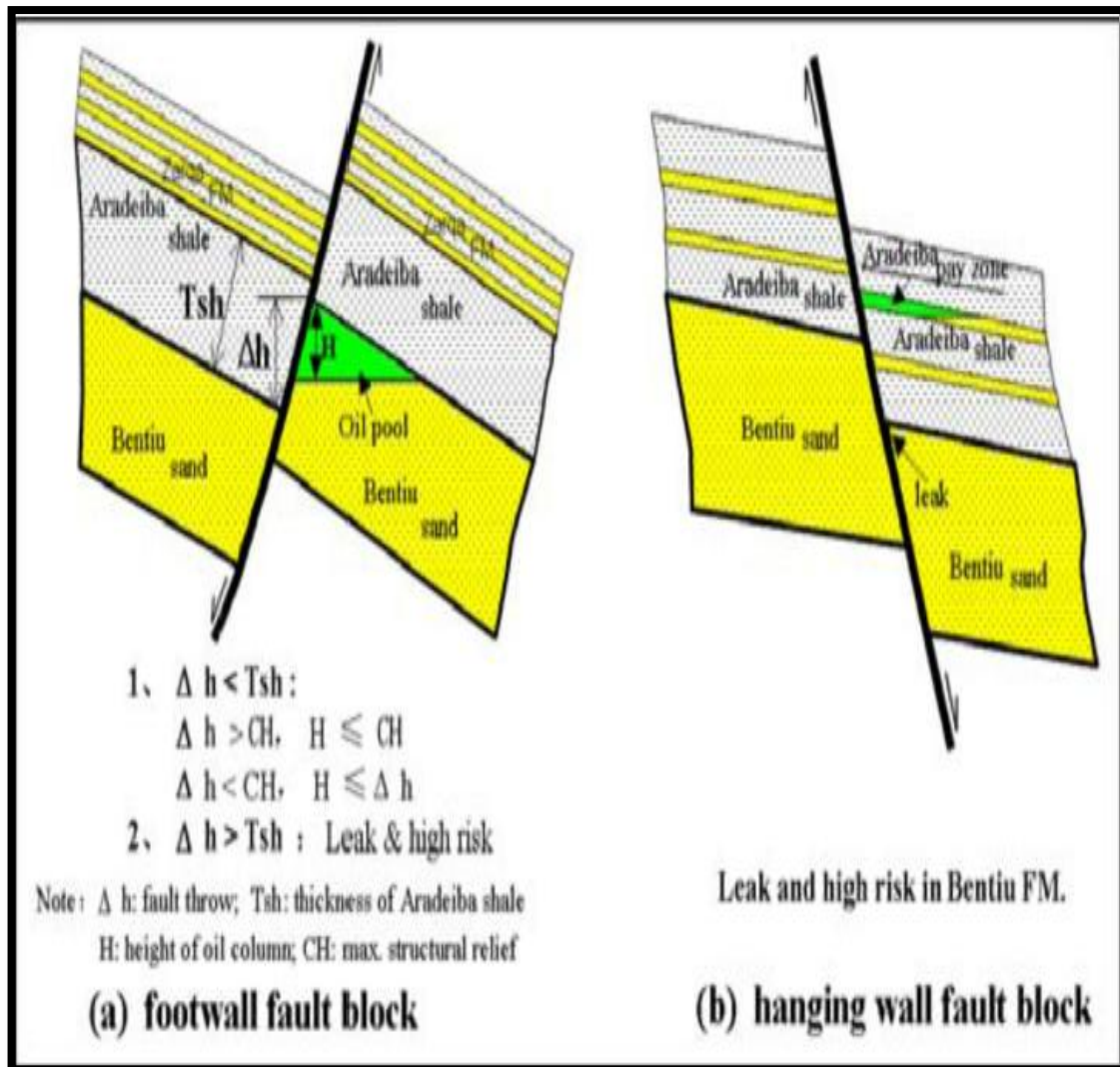


Figure (1-6). Schematic illustration of lateral seal dependence on the Aradeiba thickness, lithology, and the amount of fault throw. (a) Footwall block; fault throw is less than the thickness of Aradeiba Shale, massive Aradeiba Shale provides the top and lateral seal for Bentiu reservoir. Oil column increases with increasing fault throw. Where fault throw is larger than the thickness of Aradeiba Shale, Bentiu objective is juxtaposed against Zarqa sand, resulting in lateral seal failure. (b) Hanging wall fault block; Aradeiba intraformational shale and fault smear provide the top and lateral seal for Aradeiba reservoirs; for Bentiu Sand, the objective is juxtaposed against the Bentiu massive sand across fault causing lateral seal failure. However, fault smear can provide weak lateral seal to form a limited oil column.

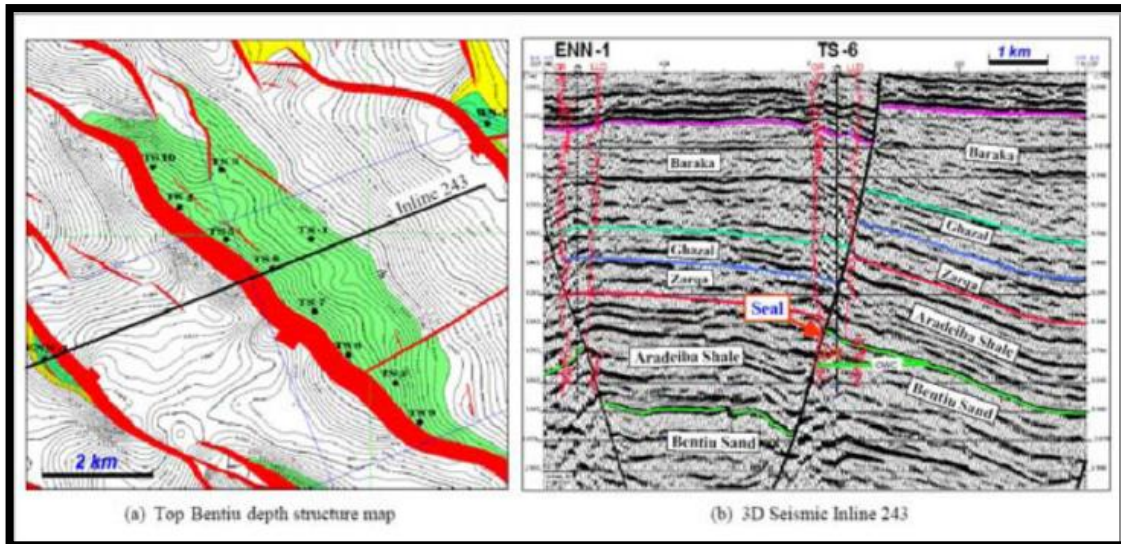


Figure (1-7). An excellent fault-sealing example. (a) The top Bentiu depth map shows a field charged to structural spill point with 140-m oil column. (b) 3D seismic section illustrates that the thick massive Aradeiba Shale (480 m) provided good top and lateral seal for Bentiu reservoir. The fault throw (430 m) is less than the thickness of Aradeiba Shale.

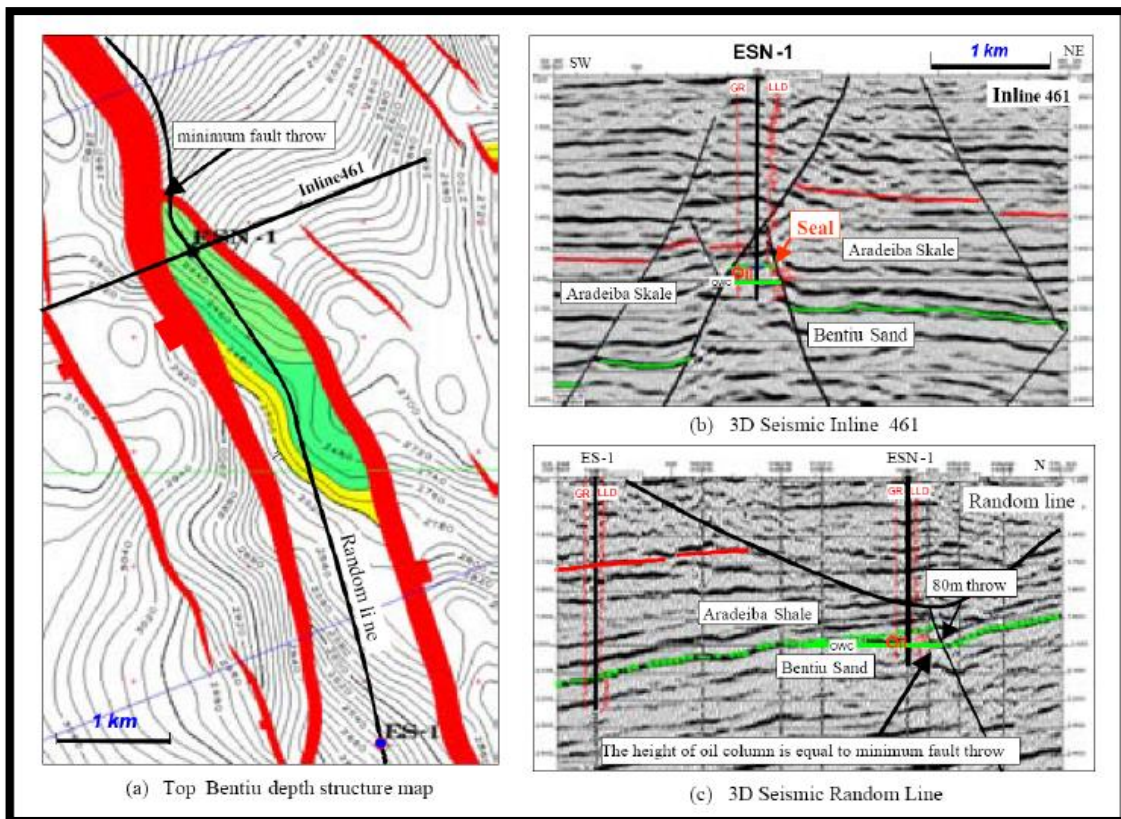


Figure (1-8). Another excellent fault-seal example. (a) Oil column is controlled by the fault throw in the northern part. (b) The thick (approximately 400 m) massive

Aradeiba Shale provided good top and lateral seal for Bentiu reservoir. (c) 3D random section illustrates that the oil column is nearly equal to minimum fault throw (80 m) at which point sand is juxtaposed sand. Figure (1-8). (a) Top Bentiu TWT map shows a tilted footwall fault block with US-1, water-bearing well, in Bentiu, and USS-1 an oil discovery well. The throw of the bounding fault varies from 400 m in the north (across US-1) to 300 m in the south (across USS-1). (b) The section illustrates that the fault throw across US-1 well is larger than the thickness of Aradeiba shale (360m), juxtaposing Bentiu reservoir against Zarqa sands, resulting in lateral leakage; hence, Bentiu sand is water-bearing. (c) The section illustrates that the fault throw is smaller than thickness of Aradeiba shale and thereby provides good lateral seal, resulting in USS-1 discovery (drilled after US-1).

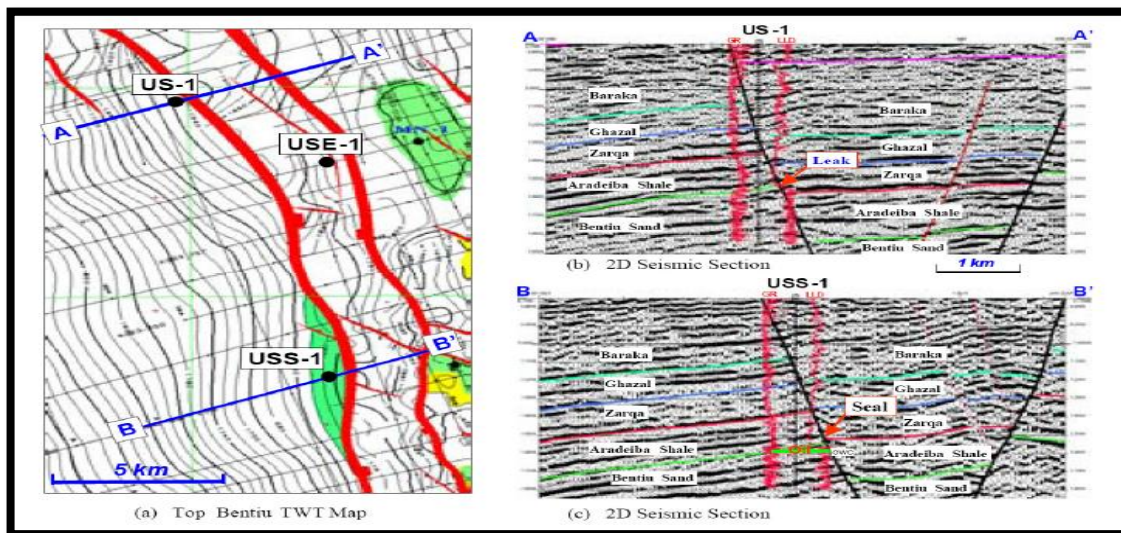


Figure (1-9). (a) Top Bentiu TWT map shows a tilted footwall fault block with US-1, water-bearing well, in Bentiu, and USS-1 an oil discovery well. The throw of the bounding fault varies from 400 m in the north (across US-1) to 300 m in the south (across USS-1). (b) The section illustrates that the fault throw across US-1 well is larger than the thickness of Aradeiba shale (360m), juxtaposing Bentiu reservoir against Zarqa sands, resulting in lateral leakage; hence, Bentiu sand is water-bearing. (c) The section illustrates that the fault throw is smaller than thickness of Aradeiba shale and thereby provides good lateral seal, resulting in USS-1 discovery (drilled after US-1).

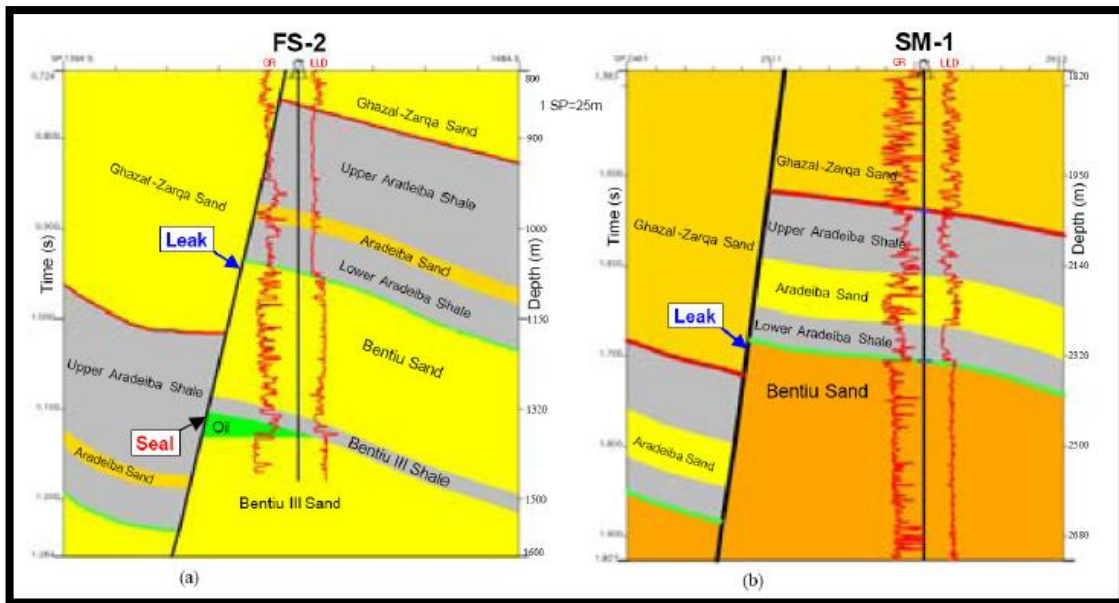


Figure (1-10). (a) Cross-section showing water-bearing zones in upper part of Bentiu reservoir, due to lateral seal failure, and pay zone in lower part (Bentiu III sand). Bentiu III sand is juxtaposed against Aradeiba Shale resulting in good lateral seal. Top seal is provided by intra-Bentiu shale. (b) Cross-section with dry hole, where there is lack of lateral seal for Bentiu reservoir. These two cross-sections illustrate lateral-seal risk associated with footwall closures. Optimum fault throw in comparison with Aradeiba Shale section is critical for trap integrity

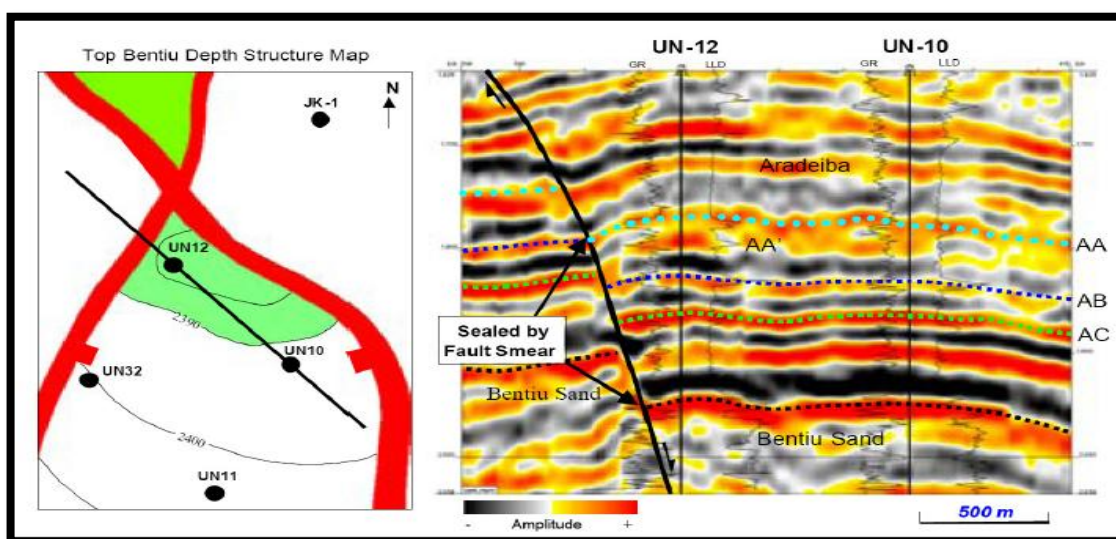


Figure (1-11). Example of oil discovery in a hanging-wall fault block. AA, AB, and AC sands are

production zones with more than 50-m oil columns. AB and AC sands juxtaposed against Aradeiba intraformational shale across the fault to provide good lateral seal; AA and Bentiu sand juxtaposed against AB sand and Bentiu massive sand, respectively, but shale fault smear provided good lateral seal, resulting in a small oil column in Bentiu reservoir.

Chapter 2

Porosity & Permeability

Chapter 2

Petrophysics is the study of the physical properties of rock . For rock to form a reservoir .(R. cosse,1993).

- 1- It must have a certain storage capacity: this property is characterized by the porosity.
- 2- The fluid must be able to flow in the rock: this property is characterized by the permeability.
- 3- It must contain a sufficient quantity of hydrocarbon, with sufficient concentration: the impregnated volume is a factor here, as well as the saturation.

2.1. Porosity

2.1.1. Introduction:

The *porosity* of a rock is the fraction of the volume of space between the solid particles of the rock to the total rock volume. The space includes all pores, cracks, vugs, inter- and intra-crystalline spaces. The porosity is conventionally given the symbol f , and is expressed either as a fraction varying between 0 and 1, or a percentage varying between 0% and 100%. Sometimes porosity is expressed in 'porosity units', which are the same as percent (i.e., 100 porosity units (pu) = 100%).

However, the fractional form is **ALWAYS** used in calculations. Porosity is calculated using the relationship. (Glover, 2001).

$$\phi = \frac{V_{pore}}{V_{bulk}} = \frac{V_{bulk} - V_{matrix}}{V_{bulk}} = \frac{V_{bulk} - (W_{dry} / \rho_{matrix})}{V_{bulk}} \dots (2-1)$$

Where:

V_{pore} = pore volume.

V_{bulk} = bulk rock volume.

V_{matrix} = volume of solid particles composing the rock matrix.

W_{dry} = total dry weight of the rock.

R_{matrix} = mean density of the matrix minerals.

It should be noted that the porosity does not give any information concerning pore sizes, their distribution, and their degree of connectivity. Thus, rocks of the same porosity can have widely different physical properties. An example of this might be a carbonate rock and sandstone. Each could have a porosity of 0.2, but carbonate pores are often much unconnected resulting in its permeability being much lower than that of the sandstone.

The porosity of interest to the reservoir specialist, that which allows the fluids in the pores to circulate, is the effective porosity ϕ_u , which corresponds to the pore connected to each other and to other formation. Also defined is the total porosity ϕ_t , corresponding to all the pores, whether interconnected or not and the residual porosity ϕ_r , which only takes account of isolated pores.

$$\phi_t = \phi_u + \phi_r \dots (2-2)$$

The effective porosity of rocks varies between less than 1% and over 40% it is often stated that the porosity is:

- 1- Low if $\phi < 5\%$.
- 2- Mediocre if $5\% < \phi < 10\%$.
- 3- Average if $10\% < \phi < 20\%$.
- 4- Good if $20\% < \phi < 30\%$.
- 5- Excellent if $\phi > 30\%$.

A distinction is made between intergranular porosity, dissolution porosity (as in limestones, for example), and fracture porosity. For fractured rocks the fracture porosity related to the rock volume is often much less than 1%. As a rule, porosity decreases with increasing depth. (R. cosse,1993).

2.1.2. Porosity Types:

Interparticle Porosity Also called "intergranular" is the predominant type found in sucrose (sugar-like) rock. Pore sizes are of the same order of magnitude as, but usually less than particular sizes. For uniform spherical grains, interparticle porosity range from 47.6% (cubic staking) to 25.9% (close pack). Intraparticle Porosity is revealed by the SEM (Scanner Electronic Microscope).it is the pore space network within the grains. A significant amount of intraparticle porosity containing connate water is nearly impervious.

Fracture Porosity Is encountered in fractured reservoirs usually observed in carbonates. The media is then defined as a double porosity media: matrix and fractures.

Fractures occur in crystalline or amorphous rock, which have no "grain size", the following figure show different type of porosity figure (2-1). (Glover, 2001).

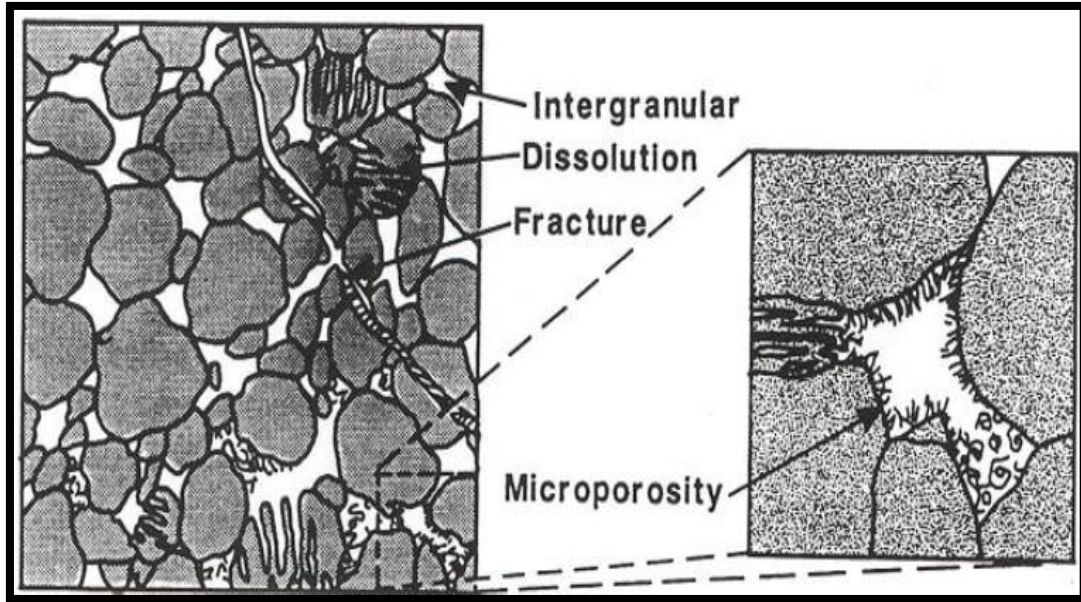


Figure (2-1) different type of porosity (Glover, 2001)

2.1.3. The Range of Porosity Values in Nature:

Table (2-1) the range of porosity values for rocks (Glover, 2001)

Lithology	Porosity Range (%)
Unconsolidated sands	35-45
‘Reservoir’ Sandstones	15-35
Compact Sandstones	5-15
Shale	0-45
Clays	0-45
Massive Limestone	5-10
Vuggy Limestone	10-40
Dolomite	10-30

Chalk	5-40
Granite	<1
Basalt	<0.5
Gneiss	<2
Conglomerate	1-15

2.1.4. Porosity Logs:

In any reservoir, we need to have a certain amount of open space so that hydrocarbons have some where to exist. We call this storage space porosity, and typically use three basic tools to determine what porosity (ϕ) might be. These are the Neutron tool, the Density tool, and the sonic tool. While all of these tools give a porosity output, they only infer this from different properties of the rock and fluid in the rock. (Glover, 2001).

2.1.4.1. The Sonic Log

The Sonic log, as the name implies, uses the travel time of sound through the formation to infer porosity. That is, it sends a sound pulse or a 'click' out from a transmitter, and then measures the time it takes to travel through the formation and back to a receiver on the tool. By comparing how fast the 'click' travels through the rock to how fast it should travel if there were no porosity, and knowing how fast sound will travel through fluid, we can infer a liquid filled porosity. Since sound travels at different speeds through different types of rock, it is important to know rock type (sandstone, limestone, or dolomite). Also, it is important to note that whatever is in the pore space (porosity) will also have a small affect on the porosity (for example, sound travels through gas at lower rates than through fluid, therefore porosity estimates in gas will appear high). The equation for finding porosity (commonly we use the Wyllie Time-Average Equation which is based on laboratory measurements) is a follows

$$\phi = (t_{LOG} - t_{ma}) / (t_{fl} - t_{ma}) \dots(2-3)$$

Where:

ϕ = porosity

t_{LOG} = sonic travel time read from the log

t_{ma} = sonic travel time in a clean 0 porosity matrix

t_{fl} = sonic travel time in the wellbore fluid

Some common values for sonic travel times (Dt) are:

Sand Dt = 182 ms/m

Limestone Dt = 156 ms/m

Dolomite Dt = 143 ms/m

Anhydrite Dt = 164 ms/m

Fresh mud's Dt = 620 ms/m

2.1.4.2 The Neutron Log

The second porosity tool we will look at is the Neutron porosity tool. The neutron tool uses the amount of hydrogen in a formation to infer porosity. Since water / oil has a relatively constant amount of hydrogen atoms by volume, the amount of hydrogen can be used to infer the amount of fluid in a formation, which in a clean formation is the porosity.

2.1.4.3 The Density Log

The third common type of porosity tool is the Density tool. The density tool, as its name implies, uses the electron density of the formation to infer a porosity. It makes use of a radioactive source which emits medium energy gamma rays into the formation. The amount of number of gamma rays that are received at the detector indicates the formation density. This density that the tool reads is a combination of the density of the matrix (solid portion of the formation), the porosity of the formation, and the density of the fluid in the pore space. So, for a clean formation of known matrix density (ρ_{ma}), and having porosity (F) that contains a fluid of density (ρ_f), the formation bulk density (ρ_b) will be:

$$\rho_b = \phi\rho_f + (1-\phi)\rho_{ma} \dots (2-4)$$

Or, re writing this for porosity, we can use:

$$\phi_D = \rho_{ma} - \rho_b / \rho_{ma} - \rho_{fl} \dots (2-5)$$

Where:

ϕ_D = Density porosity.

ρ_{ma} = density of matrix material.

ρ_b = measured by density tool.

ρ_{fl} = density of fluid in the borehole

Some common Densities (ρ) are:

Sandstone - 2650 Kg/m³

Limestone - 2710 Kg/m³

Dolomite - 2870 Kg/m³

Fresh Water - 1000 Kg/m³

Oil - 850 Kg/m³

2.1.5. Total Porosity Determination:

We have now seen that the basic porosity measurements are inferred from measurements of bulk density, hydrogen concentration, and acoustic travel time. This porosity's are valid under the following conditions:

- The porosity type is intergranular, not fractured or secondary
- The matrix type is known and constant
- The rock is clean (I.e. no shale present)
- The porosity is filled with fluid

If any one of these conditions are not met, the porosity measurements will disagree in one fashion or another. This difference can be used to determine a number of factors including: lithology, primary/secondary porosity, gas vs. liquid filled porosity, etc. (Glover, 2001).

2.1.6. Calculating The Porosity:

Porosity should be calculated from the density log using the equation (Glover, 2001).

$$\phi = (\rho_m - \text{density}) / (\rho_m - \rho_f) \dots (2-6)$$

Where:

ρ_m = matrix density (in g/cc) and ρ_f = fluid density (in g/cc)

2.1.7. Porosity by Coring:

The best way of determining porosity is to carry out experiments on core extracted from the well. The basic techniques will be described here. It should be noted that

core determined porosities have a much higher degree of accuracy than porosities determined from down-hole tools, but suffer from sampling problems. Taken together core and borehole determined porosities optimize accuracy and high resolution sampling. (Glover, 2001).

There are at least 4 common methods of measuring the porosity of a core. These are:

- 1- Buoyancy.
- 2- Helium porosimetry.
- 3- Fluid saturation.
- 4- Mercury porosimetry.

2.2. Permeability

2.2.1. Definition and theory:

The term permeability has been adopted as a measurement of the porous rock's ability to conduct fluid. The measurement of permeability is the measurement of the fluid conductivity of the particular material.(J.P.Roy,2007).

Permeability characterizes the ability of rocks to allow the circulation of fluids contained in their pores.

The fundamental physical law which governs this is called the Navier-Stokes equation, and it is very complex. For the purposes of flow in rocks we can usually assume that the flow is laminar, and this assumption allows great simplification in the equations.

It should also be noted that the permeability to a single fluid is different to the permeability where more than one fluid phase is flowing. When there are two or more immiscible fluid phases flowing we use relative permeability.

The fluid flow through a cylindrical tube is expressed by Poiseuille's equation, which is a simplification of Navier-Stokes equation for the particular geometry, laminar flow, and incompressible fluids. (Glover, 2001).This equation can be written as:

$$Q = \frac{\pi r^4 (P_i - P_o)}{8 L \mu} \dots (2-7)$$

Where:

Q= the flow rate (cm^3/s or m^3/s).

r= the radius of the tube (cm or m).

P_o= the outlet fluid pressure ($dynes/cm^2$ or pa).

P_i= the inlet fluid pressure ($dynes/cm^2$ or Pa).

L= the dynamic viscosity of the fluid (poise or pa.s).

μ=the length of the tube (cm or m).

About 150 years ago Darcy carried out simple experiments on packs of sand, and hence developed an empirical formula that remains the main permeability formula in use in the oil industry today.

Darcy's formula can be expressed as:

$$Q = \frac{K A (P_i - P_o)}{L \mu} \dots (2-8)$$

Where:

Q= the flow rate (cm^3/s or m^3/s).

P= the outlet fluid pressure ($dynes/cm^2$ or pa).

P= the inlet fluid pressure ($dynes/cm^2$ or Pa).

K= the dynamic viscosity of the fluid (poise or pa.s).

A=the area of the sample (Darcy or m^2).

L=the length of tube (cm or m).

μ= the length of the tube (cm or m).

2.2.2. Controls on Permeability and the Range of Permeability Values in Nature:

Intuitively, it is clear that permeability will depend on porosity; the higher the porosity the higher the permeability. However, permeability also depends upon the connectivity of the pore spaces, in order that a pathway for fluid flow is possible. The connectivity of the pores depends upon many factors including the size and shape of grains, the grain size distribution, and other factors such as the operation of capillary forces that depend upon the wetting properties of the rock.

However, we can make some generalizations if all other factors are held constant:

- The higher the porosity, the higher the permeability.
- The smaller the grains, the smaller the pores and pore throats, the lower the permeability.
- The smaller the grain size, the larger the exposed surface area to the flowing fluid, which leads to larger friction between the fluid and the rock, and hence lower permeability.
- The permeability of rocks varies enormously, from 1 nanodarcy, nD (1×10^9 D) to 1 microdarcy, μ D (1×10^6 D) for granites, shale and clays that form cap-rocks or compartmentalize a reservoir, to several darcies for extremely good reservoir rocks. In general a cut-off of 1 mD is applied to reservoir rocks, below which the rock is not considered as a reservoir rock unless unusual circumstances apply (e.g., it is a fractured reservoir). For reservoir rocks permeabilities can be classified as in Table (2-2) below. (Glover, 2001).

Table (2-2) Reservoir permeability classification (Glover, 2001)

Permeability Value (mD)	Classification
<10	Fair
10-100	High
100-1000	Very high
>1000	Exceptional

2.2.3. Permeability Determination:

Permeability is measured on cores in the laboratory by flowing a fluid of known viscosity through a core sample of known dimensions at a set rate, and measuring the pressure drop across the core, or by setting the fluid to flow at a set pressure difference, and measuring the flow rate produced. (Glover, 2001).

2.2.4. Type of Permeability:

Relative Permeability depends upon many factors. Perhaps not surprisingly, one of those factors is the degree to which the available pore space is saturated with the flowing fluid. The pore space may not be completely saturated with one fluid but contain two or more. For, example, there may be, and generally is, both oil and water in the pores. What is more, they may both be flowing at different rates at the same time. Clearly, the individual permeability's of each of the fluids will be different from each other and not the same as the permeability of the rock with a single fluid present. These permeability's depend upon the rock properties, but also on the saturations, distributions, and properties of each of the fluids.

If the rock contains one fluid, the rock permeability is maximum, and this value is called the *absolute permeability*.

If there are two fluids present, the permeability's of each fluid depend upon the saturation of each fluid, and can be plotted against the saturation of the fluid, These are called *effective permeability's*.

Both effective permeability's are always less than the absolute permeability of the rock and their sum is also always less than the absolute permeability of the rock. The individual effective permeability's are most often expressed as a fraction of the absolute permeability of the rock to either of the two fluids when present at 100% saturation, and these are called *relative permeability's*.

Absolute Permeability Initially the Darcy work was carried out to describe the flow of one fluid (water) saturating 100% of porous media (water). The permeability to a particular fluid is independent of the fluid properties (viscosity) Therefore; the permeability to a 100% saturating fluid is a constant and characteristic of the porous media that is called the absolute permeability or specific permeability. (Glover, 2001).

2.2.5. Permeability Relationships:

The complexity of the relationship between permeability and pore geometry has resulted in much research. No fundamental law linking the two has been found. Instead, we have a plethora of empirical approximations for calculating permeability, some of which are given in Table (2-3). (Glover, 2001).

Table (2-3) empirical approximations for calculating permeability

Name	Equation	Notes
Solution Channel	$k = 0.2 \times 10^8 \times d^2$	k = permeability (D) d = channel diameter (inches)
Fractures	$k = \frac{0.544 \times 10^8 \times w^3}{h}$	k = permeability (D) h = fracture width (inches) w = fracture aperture (inches)
Wyllie and Rose equations I	$k = \left(\frac{100 \phi^{2.25}}{S_{wi}} \right)^2$	k = permeability (mD) ϕ = porosity (fraction) S_{wi} = irreducible water saturation (fraction)
Wyllie and Rose equations II	$k = \left(\frac{100 \phi^2 [1 - S_{wi}]}{S_{wi}} \right)^2$	k = permeability (mD) ϕ = porosity (fraction) S_{wi} = irreducible water saturation (fraction)
Timur equation	$k = \frac{0.136 \phi^{4.4}}{S_{wi}^2}$	k = permeability (mD) ϕ = porosity (%) S_{wi} = irreducible water saturation (%)
Morris and Biggs equation	$k = \left(\frac{C \phi^3}{S_{wi}^2} \right)$	k = permeability (mD) ϕ = porosity (fraction) S_{wi} = irreducible water saturation (fraction) C = constant; oil=250; gas=80
Slichter equation	$k = \frac{10.2 d^2}{K_s}$	k = permeability (mD) d = median grain size (microns) K_s = packing correction; slope of line when plotting median grain size vs. permeability.
Kozeny-Carman equation	$k = \frac{c d^2 \phi^3}{(1 - \phi)^2}$	k = permeability (mD) ϕ = porosity (fraction) c = constant d = median grain size (microns)
Berg equation	$k = 8.4 \times 10^{-2} \times d^2 \phi^{5.1}$	k = permeability (mD) ϕ = porosity (fraction) d = median grain size (microns)
Van Baaren equation	$k = 10 D_d^2 \phi^{(3.64+m)} C^{-3.64}$	k = permeability (mD) ϕ = porosity (fraction) D_d = modal grain size (microns) C = sorting index m = Archie cementation exponent.
RGPZ equation	$k = \frac{1000 d^2 \phi^{3m}}{4 a m^2}$	k = permeability (mD) d = weighted geometric mean grain size (microns) ϕ = porosity (fraction) m = Archie cementation exponent. a = grain packing constant

2.3. PoroPerm Relationships

The most obvious control on permeability is porosity. This is because larger porosities mean that there are many more and broader pathways for fluid flow. Almost invariably, a plot of permeability (on a logarithmic scale) against porosity for a formation results in a clear trend with a degree of scatter associated with the other influences controlling the permeability. For the best results these poroperm cross-plots should be constructed for clearly defined lithologies or reservoir zones. If a cross-plot is constructed for a whole well with widely varying lithologies, the result is often a disappointing cloud of data in which the individual trends are not apparent.

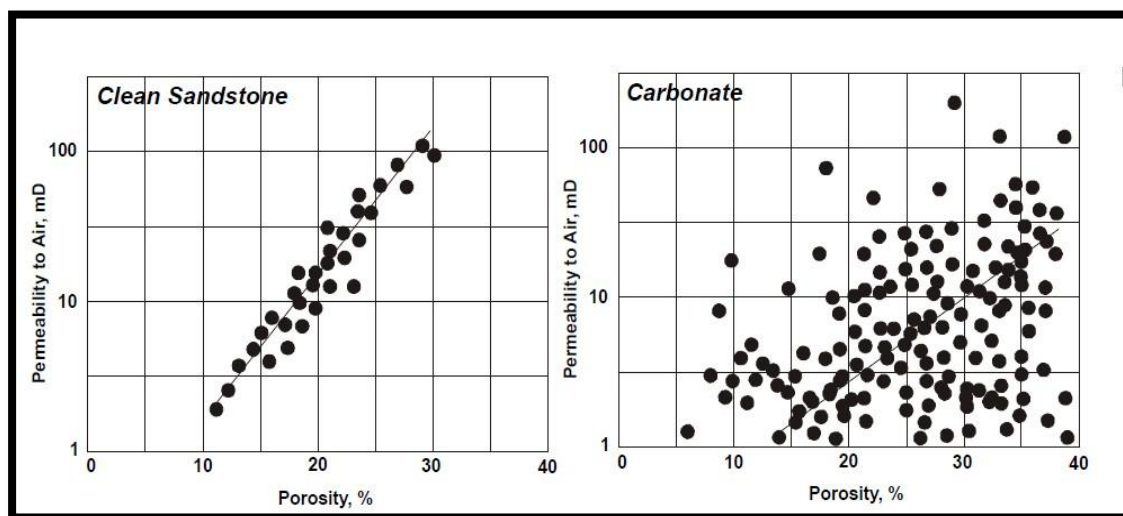


Figure (2-2) shows a poroperm cross-plot for clean sandstone and a carbonate.

Figure (2-2) poroperm cross-plot for clean sandstone and a carbonate(Glover, 2001)

It is clear from this figure that the permeability of the sandstone is extremely well controlled by the porosity (although usually there is more scatter than in this figure), whereas the carbonate has a more diffuse cloud indicating that porosity has an influence, but there are other major factors controlling the permeability. In the case of carbonates (and some volcanic rocks such as pumice), there can exist high porosities that do not give rise to high permeabilities because the connectivity of the vugs that make up the pore spaces are poorly connected.

Poroperm trends for different lithologies can be plotted together, and form a map of poroperm relationships, as shown in Figure (2-3) below. It would be time consuming to describe the figure in detail, but interpretation is not difficult. For example, fractured rocks fall above the sandstones because their porosity (fracture

porosity) is very low, yet these fractures form very connected networks that allow the efficient passage of fluids, and hence the permeability is high. Such permeability may be directional because of preferred orientations of the fractures. By comparison, clay cemented sandstones have high porosities, but the porosity is mainly in the form of micro-porosity filled with chemically and physically (capillary) bound water which is immobile. This porosity does not take place in fluid flow, so the permeability is low.

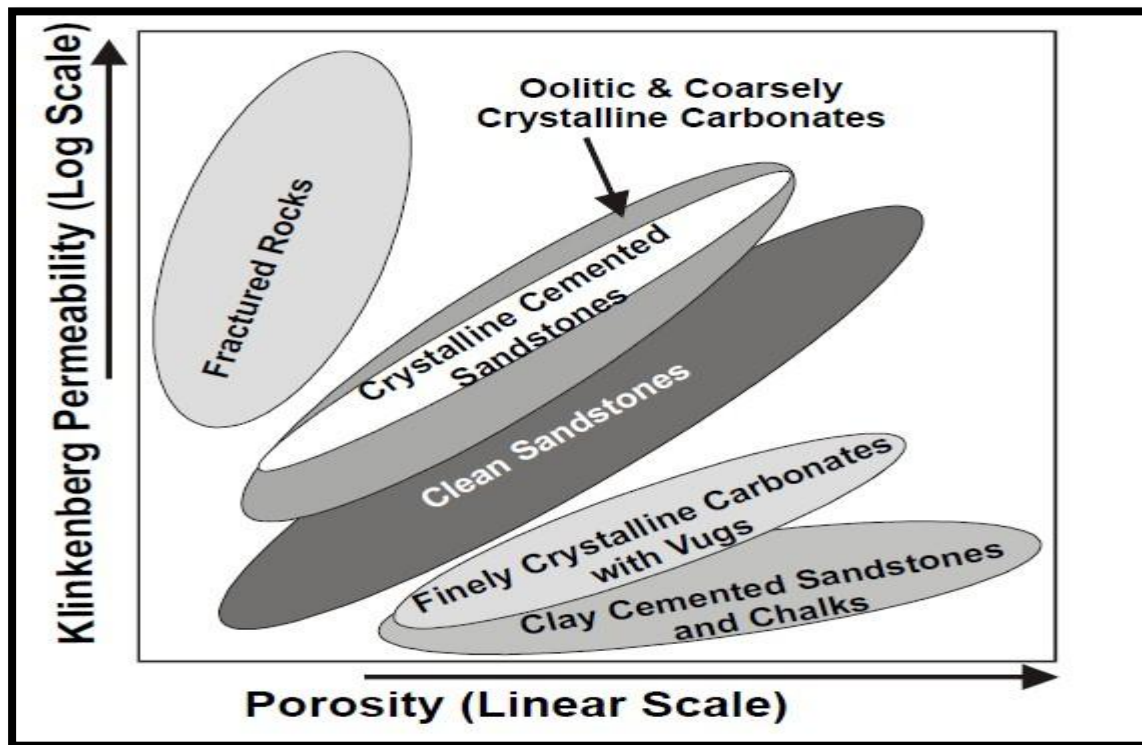


Figure (2-3) Poroperm relationships (Glover, 2001)

It might be expected that grain size also has some control on permeability. Figure (2-4) shows a poroperm cross-plot for a well in a carbonate reservoir where the grain size, porosity and permeability were measured for each core taken. Taking the data as a whole, there is little in the way of a clear trend. However, trends emerge when the individual grain size fractions are considered. Now it is clear that rocks with smaller grain sizes have smaller permeabilities than those with larger grain sizes. This is because smaller grain sizes produce smaller pores, and rather more importantly, smaller pore throats, which constrain the fluid flow more than larger grains which produce larger pore throats.

In summary, permeability:

- Depends upon porosity.

- Depends upon the connectivity of the flow paths in the rock.
 - Depends, therefore, in a complex way upon the pore geometry of the rock.
- Is a directional quantity that can be affected by heterogeneous or directional properties of the pore geometry. (Glover, 2001).

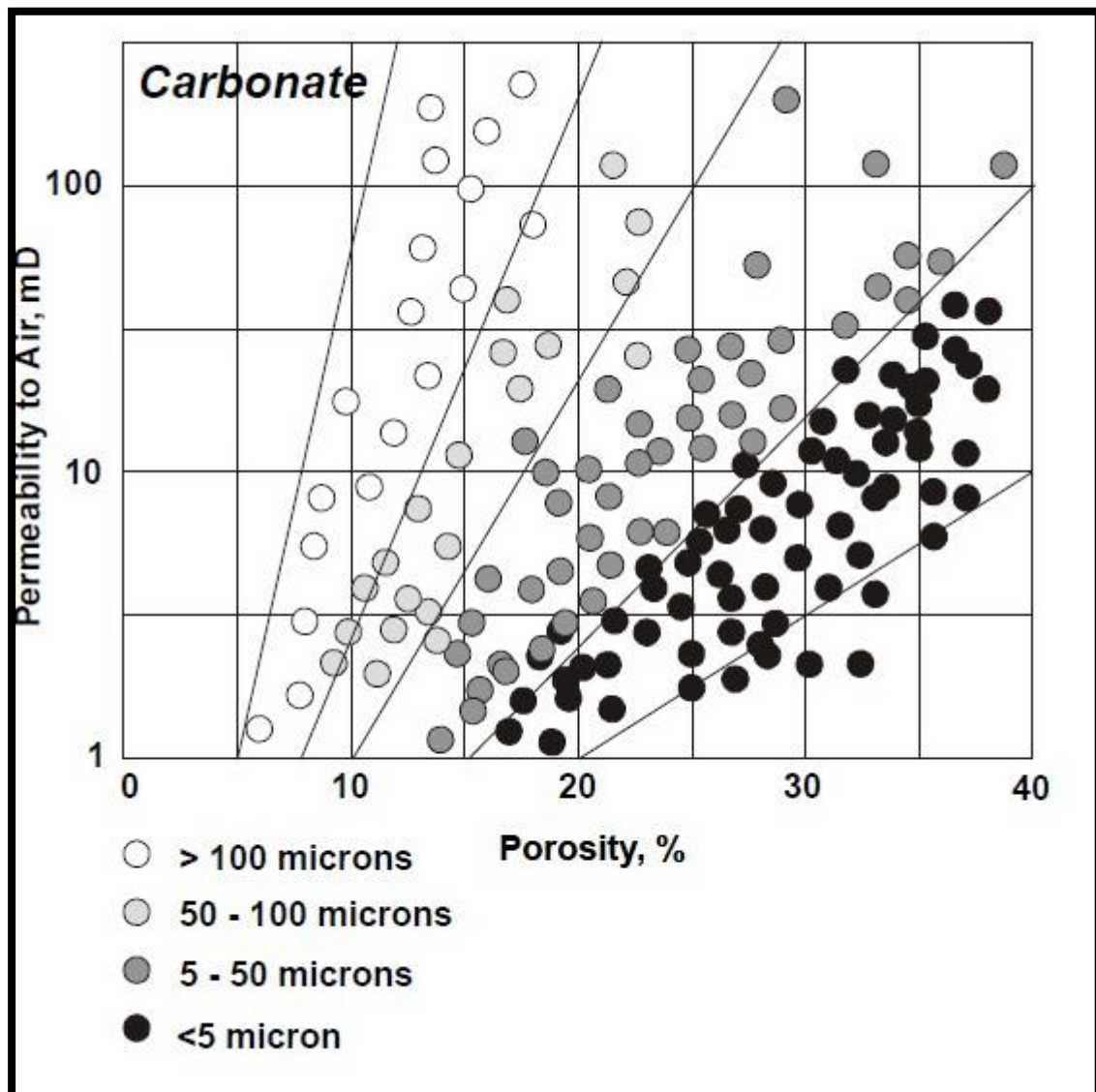


Figure (2-4) Poroperm cross-plots and the influence of grain size. (Glover, 2001)

Chapter 3

Pressure & Saturation

CHAPTER 3

This chapter will present the origins of pore pressure and principles its determinations and fluid saturation.

hence the emphasis will be placed on the practical utilization of pore pressure in the well planning process; it is hoped that the ideas will help to better understand lithological columns and deduce potential hole problems before producing a final well plan (knowledge of formation pressures is vital to the safe planning of a well).

Accurate values of formation pressures are used to design safe mud weights to overcome fracturing the formation and prevent well kicks. The process of designing and selection of casing weights/grades is predominately dependent on the utilization of accurate values of formation pressure. Cementing design, kick control, selection of wellhead and Xmas trees and even the rig rating are dependent on the formation pressures encountered in the well.

All formations penetrated during the drilling of a well contain pressure which may vary in magnitude depending on depth, location and proximity to other structures. In order to understand the nature, extent and origin of formation pressures, it is necessary to define and explain basic wellbore pressure concepts. (H.Rabia,2001)

3.1. Hydrostatic Pressure:

Hydrostatic pressure is defined as the pressure exerted by a column of fluid. Mathematically, hydrostatic pressure is expressed as (H.Rabia,2001)

$$HP = g \times \rho_f \times D \dots (3-1)$$

Where:

HP = hydrostatic pressure

g = gravitational acceleration

ρ_f = average fluid density

D = true vertical depth or height of the column

In field operations, the fluid density is usually expressed in pounds/gallon (ppg), psi/foot, pounds/cubic foot (ppf) or as specific gravity (SG). In the Imperial system of units, when fluid density is expressed in ppg and depth in feet, the hydrostatic pressure is expressed in psi (lb/in²):

$$HP \text{ (psi)} = 0.052 \times \rho_f \text{ (ppg)} \times D \text{ (ft)} \dots (3-2)$$

For the purposes of interpretation, all wellbore pressures, such as formation pressure, fracture pressure, fluid density and overburden pressure, are measured in terms of hydrostatic pressure.

3.2. Overburden Pressure:

The overburden pressure is defined as the pressure exerted by the total weight of overlying formations above the point of interest. The total weight is the combined weight of both the formation solids (rock matrix) and formation fluids in the pore space. The density of the combined weight is referred to as the bulk density (ρ_b). The overburden pressure can therefore be expressed as the hydrostatic pressure exerted by all materials overlying the depth of interest (H.Rabia,2001)

$$\sigma_{ov} = 0.052 \times \rho_b \times D \dots (3-3)$$

Where:

σ_{ov} = overburden pressure (psi) ρ_b = formation bulk density (ppg)

D = true vertical depth (ft)

And similarly as a gradient (EMW) in ppg:

$$\sigma_{ovg} = \frac{0.433}{0.052} \rho_b \dots (3-4)$$

σ_{ovg} = overburden gradient, ppg

ρ_b = formation bulk density (gm/cc).

(The factor 0.433 converts bulk density from gm/cc to psi/ft).

3.3. Pore Pressure:

Pore pressure is defined as the pressure acting on the fluids in the pore spaces of the rock. This is the scientific meaning of what is generally referred to as formation (pore) pressure. Depending on the magnitude of pore pressure, it can be described as being normal, abnormal or subnormal. (H.Rabia,2001)

3.3.1. Normal Pore Pressure:

Normal pore pressure is equal to the hydrostatic pressure of a column of formation fluid extending from the surface to the subsurface formation being considered. In other words, if the formation was opened up and allowed to fill a column whose length is equal to the depth of the formation then the pressure at the bottom of the column will be equal to the formation pressure and the pressure at surface is equal to zero. Normal pore pressure is not a constant. The magnitude of normal pore pressure varies with the concentration of dissolved salts, type of fluid, gases present and temperature gradient. For example, as the concentration of dissolved salts increases the magnitude of normal pore pressure increases.

3.3.2. Abnormal Pore Pressure:

Abnormal pore pressure is defined as any pore pressure that is greater than the hydrostatic pressure of the formation water occupying the pore space. Abnormal pressure can be thought of as being made up of a normal hydrostatic component plus an extra amount of pressure. Abnormal pore pressure can occur at any depth ranging from only a few hundred feet to depths exceeding 25,000 ft. The cause of abnormal pore pressure is attributed to a combination of various geological, geochemical, geothermal and mechanical changes. However for any abnormal pressure to develop there has to be an interruption to or disturbance of the normal compaction and de-watering process.

3.3.3. Subnormal Pore Pressure:

Subnormal pore pressure is defined as any formation pressure that is less than the corresponding fluid hydrostatic pressure at a given depth. Subnormal pore pressures are encountered less frequently than abnormal pore pressures and are often developed long after the formation is deposited. Subnormal pressures may have natural causes related to the stratigraphic, tectonic and geochemical history of an area, or may have been caused artificially by the production of reservoir fluids. The Rough field in the Southern North Sea is an example of a depleted reservoir with a subnormal pressure.

3.4. Pore Pressure Evaluation:

Some of the primary methods used to predict pore pressures are enumerated as follows (H.Rabia,2001)

- 1/ Sonic log
- 2/ Resistivity log.
- 3/Density log.

3.4.1. Sonic Logs:

In general, the acoustic logs are considered to provide the most reliable quantitative estimations of pore pressure. The main benefits of acoustic logs are that they are relatively unaffected by borehole size, formation temperature and pore water salinity. The parameters that do affect the acoustic log are formation type and

compaction related effects such as porosity/density and are therefore directly applicable to pore pressure evaluation.

Theory of Sonic Logging

The sonic log measures the transit time (Δt) for a compression sonic wave to travel through the formation from transmitter to receiver. The time to travel through one foot (or one metre) is termed the Interval Transit Time (ITT). In a shale sequence showing a normal compaction profile (and therefore normal pressure); the transit time should decrease with depth due to the decreased porosity and increasing density show in figure (3.1). Abnormally pressured shale tend to have higher porosity and lower density than normally pressured shale at the same depth. Hence the ITT values will be higher.

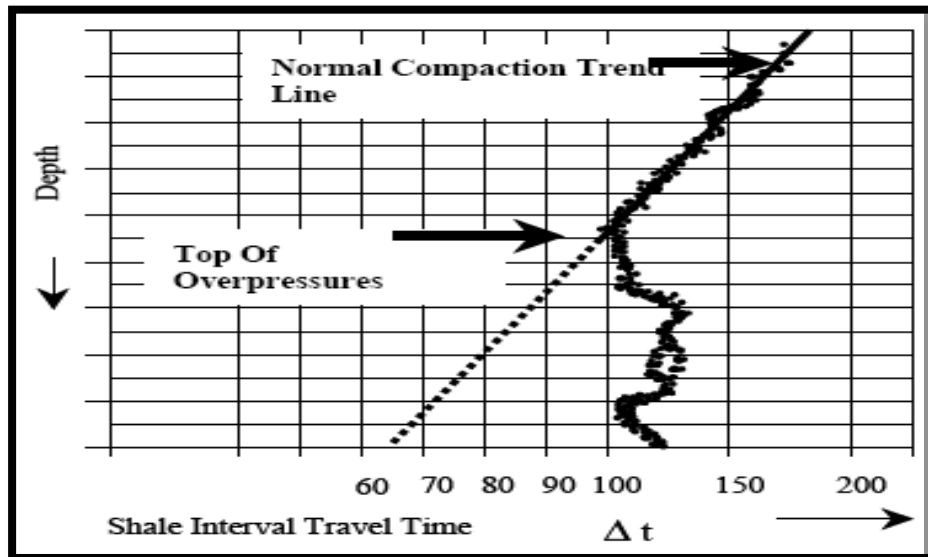


Figure (3-1) Shale interval travel time vs. depth (H.Rabia,2001)

$$pp = \sigma_{ov} - (\sigma_{ov} - P_n) \left(\frac{\Delta t_n}{\Delta t_o} \right)^3 \dots (3-5)$$

Where:

PP =Pore pressure (ppg).

σ_{ov} =Overburden (ppg).

P_n =Normal pore pressure (ppg).

Δt_n =Normal pore pressure trend line t value at depth of interest.

Δt_o =Observed t value at the depth of interest.

3.4.2. Resistivity Logs:

Shale resistivity values were obtained originally from the amplified short normal log. However, in recent years the use of deep induction logs is preferred as these enable the use of data in all types of drilling fluid and affording a greater depth of investigation. Shale resistivity increases with depth.

The resistivity (the reciprocal of conductivity) of shale depends upon the following factors:

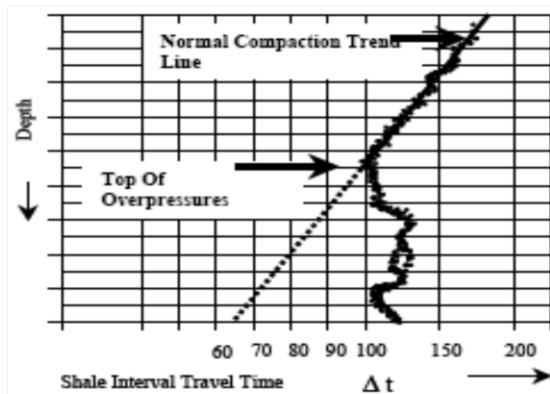
- Porosity
- Salinity of the pore water
- Temperature.

The salinity of the pore water does not normally vary greatly with depth and hence its effect is often discounted. In addition, temperature normally increases uniformly with depth and hence resistivity values can be corrected for the temperature increase. Porosity is thus the major factor affecting resistivity values.

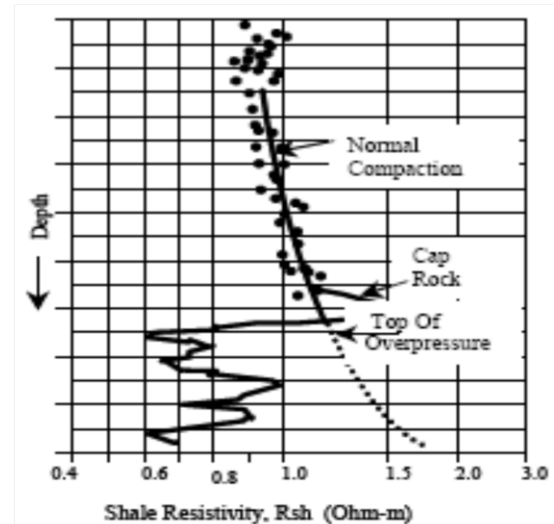
Theory of Resistivity Logging

The basic theory relies upon shale resistivity increasing with depth in normally pressured shale as the porosity decreases. An increasing porosity, and thus higher pore water content, is indicative of abnormally pressured shale and will result in lower resistivity. A logarithmic plot of shale resistivity vs. linear depth figure (3.2), is constructed. A normal pore pressure trend line is established through known normally pressured shale and thus any decrease in shale resistivity value away from the trend line indicates abnormal pore pressure. The magnitude of the abnormal pore pressure can be calculated using an Eaton type equation pressure.

Also we can plot the response of the shale point acoustic transit time to abnormal pressure show in figure (3-3).



Response Of Shale Point Acoustic
Transit Time To Abnormal Pressure



Use of shale resistivity for
abnormal pressure determination

Figure (3-2) a logarithmic plot of shale resistivity vs linear depth (H.Rabia,2001)

Figure (3-3) response of shale acoustic transit time to abnormal pressure (H.Rabia,2001)

3.4.3. Formation Density Logs:

A typical formation density logging tool consists of a radioactive source which bombards the formation with medium energy gamma rays. The gamma rays collide with electrons in the formation resulting in scattering of the gamma rays. The degree of scattering is directly related to the electron density and therefore the bulk density of the formation.

A plot of shale bulk density versus depth will show a straight line normal compaction trend line; the shale bulk density will increase with depth due to the increased compaction. This results in reduced porosity and pore water expulsion. In abnormally pressured shale, compaction is often retarded, resulting in increased porosity and thus lower density than normally pressured shale at an equivalent depth. As such a decrease in shale bulk density values from the normal compaction trend line is observed when entering a zone of abnormal pore. (H.Rabia,2001)

3.5. Saturation:

To the engineer there is important factor to be determined. What is the fluid content of the rock ? in most oil-bearing formation it is believed that the rock was completely saturated with water prior to the invasion and trapping of petroleum. The less dense hydrocarbon are considered to migrate to position of hydrostatic and dynamic equilibrium, thus displacing water from the interstices of the structurally high part of

the rock. The oil will not displace all the water which originally occupied these pores. Thus, reservoir rock normally will contain both petroleum and hydrocarbons and water (frequently referred to as connate water) occupying the same or adjacent pores. To determine the quantity of hydrocarbons accumulated. In a porous rock formation, it is necessary to determine the fluid saturation (oil, water and gas) of the rock material. (JAMES W. AMYX & others, 1988)

Fluid saturation is defined as the ratio of volume of fluid phase in given reservoir rock sample to the pore volume of the sample. In another words fluid saturation is defined as percent of the pore volume occupied by a particular fluid phase (oil & gas).

We have seen that the viability of a reservoir depends upon three critical parameters. The first two of these are the porosity of the reservoir rock, which defines the total volume available for hydrocarbon saturation, and the permeability, which defines how easy it is to extract any hydrocarbons that are present. The final critical parameter is the hydrocarbon saturation, or how much of the porosity is occupied by hydrocarbons. This and the related gas and water saturations are controlled by capillary pressure.

The important of accurate fluid saturation information can also be highlighted because hydrocarbons in place (oil & gas) are calculated on the basis of simple volumetric balance of hydrocarbons present in the effective pore space of the system. For example; if a reservoir is 50% saturation with water; this means the half of the available pore space in the reservoir actually contains oil. (Dandekar, Abhijit Y, 2006)

3.5.1. Mathematical expressions for fluid saturation:

Fluid saturation is defined as percent of the pore volume occupied by a particular fluid phase (oil & gas).

$$\text{Fluid saturation} = \frac{\text{total volume of the fluid phase}}{\text{pore volume}} \dots (3-6)$$

$$S_g = \frac{\text{volume of gas}}{\text{pore volume}} \dots (3-7)$$

$$S_w = \frac{\text{volume of water}}{\text{pore volume}} \dots (3-8)$$

$$S_o = \frac{\text{volume of oil}}{\text{pore volume}} \dots (3-9)$$

$$S_g + S_o + S_w = 1 \dots (3-10)$$

Where:

S_g = gas saturation.

S_o = oil saturation.

S_w = water saturation.

3.5.2. Methods to Determination Saturation:

There are in general two ways of measuring original fluid saturations:

The direct approach and in the direct approach. The direct approach involves either the extraction of the reservoir fluids or the leaching of the fluid from a sample of the reservoir rock. The in direct approach relies on a measurement of some other property, such as capillary pressure, and the derivation of a mathematical relationship between the measured property and saturation .

Direct methods include retorting the fluids from the rock, distilling the fluid with a modified ASTM (American Society For Testing and Materials) procedure, and centrifuging the fluids. Each method relies on some procedure to remove the rock sample for the reservoir. Experience has found that it is difficult to remove the sample without altering the state of the fluids and/or rock. The indirect methods use logging or capillary pressure measurement. With either method, errors are built into the measurement of saturation. However, under favorable circumstances and with careful attention to detail, saturation value can be obtained within useful limit of accuracy.(B.C.Craft and M.F.Hawkins,1991).

For rock sample saturated with a fluid and surrounded by another fluid:

1-If the saturating fluid is wetting, it is displaced by the surrounding fluid only if the excess pressure applied to the surrounding fluid is at least equal to the capillary pressure for the largest pores.

2-If the saturating fluid is non-wetting, it is displaced spontaneously by the surrounding fluid. (R. cosse,1993).

Chapter 4

Calculation

Chapter 4

This chapter will review the theories and calculation effected by calculating the formation prosperities for better understanding of formation.

4.1. Porosity calculation

The base of the calculation depends on the following relationship:

4.1.1. Total porosity:

Porosity by density:

The porosity by density was calculated using equation (4-1).

$$\phi = \frac{\rho_{ma} - \rho_b}{\rho_{ma} - \rho_f} \dots (4-1)$$

Where:

ϕ = Density porosity.

ρ_{ma} = density of matrix material.

ρ_b = measured by density tool.

ρ_f = density of fluid in the borehole.

Porosity by sonic:

The porosity from sonic was calculated using equation (4-2).

$$\phi = \frac{t_{log} - t_{ma}}{t_f - t_{ma}} \dots (4-2)$$

Where:

ϕ =Sonic porosity.

t_{LOG} = sonic travel time read from the log.

t_{ma} = sonic travel time in a clean 0 porosity matrix.

t_f = sonic travel time in the wellbore fluid.

Porosity by Neutron:

Their direct methods which mean that don't need to calculate, that gives direct values of porosity.

The Neutron log is presented in porosity units based on a particular matrix type (sandstone, limestone, or dolomite).

The tables below (4-1) , (4-2) , (4-3) , (4-4) , (4-5) explain the data required to calculated total porosity from data log :

Table (4-1): log data required for Well 1:

Sand Zone	Depth M	Thickness M	Neutron V/V	Sonic μS/F	Density G/CC
1	915 – 1020.45	105.45	0.452	123.57	2.2
2	1023.45 – 1054.8	31.35	0.505	135.1	2.15
3	1068.8 – 1070.4	1.6	0.352	116.34	2.144
4	1072.05 – 1074.45	2.4	0.325	114.74	2.14

Table (4-2): log data required for Well 3:

Sand Zone	Depth M	Thickness M	Neutron V/V	Sonic μS/F	Density G/CC
1	932 – 1072.6	140.6	0.442	128.48	2.169
2	1090 – 1096.8	6.8	0.379	117.49	2.46
3	1099- 1107.5	8.5	0.367	117.32	2.176
4	1119.5 – 1123	3.5	0.462	126.74	2.79
5	1134.5 – 1186.4	51.9	0.504	141.1	2.093
6	1196.8 – 1197.89	1	0.516	150.32	2.130
7	1200 – 1202.6	1.09	0.499	112.1	2.35
8	1219.4 – 1245.7	26.3	0.440	122.1	2.73
9	1247.7 – 1261.3	13.6	0.499	112.51	2.044
10	1263.5 - 1266	2.5	0.265	101	2.288

Table (4-3): log data required for Well 4:

Sand Zone	Depth M	Thickness M	Neutron V/V	Sonic μS/F	Density G/CC
1	897.03 – 937.87	40.84	0.448	125.357	2.178
2	948 – 972.92	24.84	0.507	125.676	2.242
3	942.07 – 989.99	7.92	0.494	136.283	2.247
4	1032.1 – 1063	30.9	0.421	121.586	2.209
5	1088.3 – 1098.1	6.8	0.363	114.56	2.188
6	1211.1 – 1220	8.5	0.528	129.57	2.125
7	1251.1 – 1253.9	2.8	0.279	87.53	2.437

Table (4-4): log data required for Well 6:

Sand Zone	Depth M	Thickness M	Neutron V/V	Sonic μS/F	Density G/CC
1	900.07 – 904.95	4.85	0.444	129.84	2.042
2	911.05 – 920.95	9.9	0.440	145.31	2.077
3	991.06 – 998.98	7.92	0.440	141.876	2.081
4	1009 – 1019.9	10.9	0.422	140.868	2.07
5	1034 – 1248	250	0.487	132.035	2.136

Table (4-5): log data required for Well 7:

Sand Zone	Depth M	Thickness m	Neutron V/V	Sonic $\mu\text{S/F}$	Density G/CC
1	867 – 981.91	114.91	0.432	127.767	2.222
2	990.4 – 1058.9	68.76	0.457	117.3	2.89
3	1081.1 – 1097.9	16.8	0.362	118.813	2.96
4	1133.1 – 1140.9	7.8	0.549	133.785	2.037
5	1144 – 1154.9	9.9	0.569	133.502	1.0948
6	1205 – 1229.9	24.9	0.531	128.106	1.912
7	1261.1 – 1266.9	5.8	0.233	93.95	2.297

Determine the Porosity by density:

By using equation (4-1) where:

$$\rho_{ma}=2.65 \text{ (g/c}^3\text{)}$$

$$\rho_f=1.1 \text{ (g/c}^3\text{)}$$

Determine the Porosity by sonic:

By using equation (4-2) where:

$$t_{ma}=55.5 \text{ (}\mu\text{S/F)}$$

$$t_f=185 \text{ (}\mu\text{S/F)}$$

The tables below (4-6) , (4-7) , (4-8) , (4-9) , (4-10) explain the total porosity calculated by sonic ,density and neutron:

Total porosity:

Table (4-6): Total porosity for Well 1:

Sand Zone	Depth M	Φdensity	Φsonic	Φneutron
1	915 – 1020.45	0.289	0.525	0.452
2	1023.45 – 1054.8	0.323	0.614	0.504
3	1068.8 – 1070.4	0.326	0.47	0.351
4	1072.05 – 1074.45	0.328	0.457	0.335

Table (4-7): Total porosity for Well 3:

Sand Zone	Depth M	Φdensity	Φsonic	Φneutron
1	932 – 1072.6	0.31	0.563	0.442
2	1090 – 1096.8	0.325	0.478	0.378
3	1099- 1107.5	0.306	0.477	0.367
4	1119.5 – 1123	0.303	0.55	0.461
5	1134.5 – 1186.4	0.359	0.66	0.503
6	1196.8 – 1197.89	0.335	0.734	0.515
7	1200 – 1202.6	0.331	0.437	0.499
8	1219.4 – 1245.7	0.307	0.514	0.439
9	1247.7 – 1261.3	0.39	0.44	0.498
10	1263.5 – 1266	0.233	0.35	0.264

Table (4-8): Total porosity for Well 4:

Sand Zone	Depth M	Φdensity	Φsonic	Φneutron
1	897.03 – 937.87	0.304	0.539	0.448
2	948 – 972.92	0.263	0.541	0.507
3	942.07 – 989.99	0.26	0.592	0.494
4	1032.1 – 1063	0.284	0.51	0.421
5	1088.3 – 1098.1	0.272	0.432	0.361
6	1211.1 – 1220	0.338	0.571	0.527
7	1251.1 – 1253.9	0.137	0.247	0.278

Table (4-9): Total porosity for Well 6:

Sand Zone	Depth M	Φdensity	Φsonic	Φneutron
1	900.07 – 904.95	0.392	0.551	0.444
2	911.05 – 920.95	0.369	0.672	0.440
3	991.06 – 998.98	0.367	0.647	0.439
4	1009 – 1019.9	0.374	0.639	0.422
5	1034 – 1248	0.331	0.573	0.386

Table (4-10): Total porosity for Well 7:

Sand Zone	Depth M	Φdensity	Φsonic	Φneutron
1	867 – 981.91	0.275	0.558	0.432
2	990.4 – 1058.9	0.336	0.477	0.456
3	1081.1 – 1097.9	0.292	0.488	0.362
4	1133.1 – 1140.9	0.395	0.604	0.548
5	1144 – 1154.9	0.453	0.602	0.568
6	1205 – 1229.9	0.476	0.56	0.531
7	1261.1 – 1266.9	0.227	0.296	0.233

4.1.2. Effective Porosity:

Calculated using density-neutron combination:

$$\Phi_{eD} = \phi_D - V_{sh} * \left(\frac{\rho_{ma} - \rho_{sh}}{\rho_{ma} - \rho_f} \right) \dots (4-3)$$

Where:

ρ_{sh} = density of near shale zone.

Φ_{eD} = effective porosity from density.

V_{sh} = shale volume.

ϕ_D = Porosity from density.

$$\Phi_{eN} = \phi_N - V_{sh} \left(\frac{\rho_{ma} - \rho_{sh}}{\rho_{ma} - \rho_f} \right) \dots (4-4)$$

Φ_{eN} = effective porosity from neutron.

ϕ_N = porosity from neutron.

$$\Phi_{e\text{ COM}} = \left(\frac{\Phi_{eD} + \Phi_{eN}}{2} \right) \dots (4-5)$$

$\Phi_{e\text{ COM}}$ = Density –neutron combination.

The tables below (4-11) , (4-12) , (4-13) , (4-14) , (4-15) explain effective porosity calculated from density-neutron:

Table (4-11): Effective porosity for Well 1:

Sand Zone	Depth M	Psh	ϕ_eD	ϕ_eN	Φ_eComp
1	915 – 1020.45	2.189	0.2088	0.3771	0.292
2	1023.45 – 1054.8	2.156	0.2918	0.4439	0.317
3	1068.8 – 1070.4	2.213	0.2036	0.2288	0.216
4	1072.05 – 1074.45	2.16	0.21	0.2412	0.225

Table (4-12): Effective porosity for Well 3:

Sand Zone	Depth M	ρ_{sh}	ϕ_eD	ϕ_eN	Φ_eComp
1	932 – 1072.6	2.18	0.21	0.34	0.282
2	1090 – 1096.8	2.18	0.19	0.24	0.219
3	1099- 1107.5	2.18	0.16	0.23	0.205
4	1119.5 – 1123	2.13	0.13	0.29	0.216
5	1134.5 – 1186.4	2.06	0.2.2	0.34	0.272
6	1196.8 – 1197.89	2.16	2.17	0.35	0.264
7	1200 – 1202.6	2.21	0.21	0.37	0.295
8	1219.4 – 1245.7	2.14	0.17	0.31	0.244
9	1247.7 – 1261.3	2.29	0.238	0.39	0.336
10	1263.5 – 1266	2.29	0.14	0.17	0.16

Table (4-13): Effective porosity for Well 4:

Sand Zone	Depth M	Psh	ϕ_eD	ϕ_eN	Φ_{eComp}
1	897.03 – 937.87	2.131	0.239	0.383	0.311
2	948 – 972.92	2.235	0.184	0.429	0.306
3	942.07 – 989.99	2.167	0.121	0.355	0.238
4	1032.1 – 1063	2.207	0.18	0.321	0.252
5	1088.3 – 1098.1	2.2	0.104	0.2	0.169
6	1211.1 – 1220	2.303	0.237	0.427	0.332
7	1251.1 – 1253.9	2.303	0.007	0.149	0.078

Table (4-14): Effective porosity for Well 6:

Sand Zone	Depth M	Psh	ϕ_eD	ϕ_eN	Φ_{eComp}
1	900.07 – 904.95	2.28	0.369	0.336	0.352
2	911.05 – 920.95	2.05	0.193	0.264	0.228
3	991.06 – 998.98	2.17	0.22	0.368	0.293
4	1009 – 1019.9	2.15	0.27	0.318	0.293
5	1034 – 1248	2.15	0.257	0.312	0.284

Table (4-15): Effective porosity for Well 7:

Sand Zone	Depth M	Psh	ϕ_eD	ϕ_eN	Φ_{eComp}
1	867 – 981.91	2.189	0.193	0.350	0.277
2	990.4 – 1058.9	2.221	0.217	0.337	0.277
3	1081.1 – 1097.9	2.09	0.122	0.182	0.147
4	1133.1 – 1140.9	2.114	0.21	0.364	0.287
5	1144 – 1154.9	2.084	0.266	0.412	0.339
6	1205 – 1229.9	2.064	0.3	0.355	0.327
7	1261.1 – 1266.9	2.2	0.84	0.09	0.087

By using [surfur8 software](#) the effective porosity data calculated by using density-neutron combination used to extract contour map which illustrate the effective porosity distribution for Aradeiba formation in bamboo field for the five wells show in figure (4-1) below .

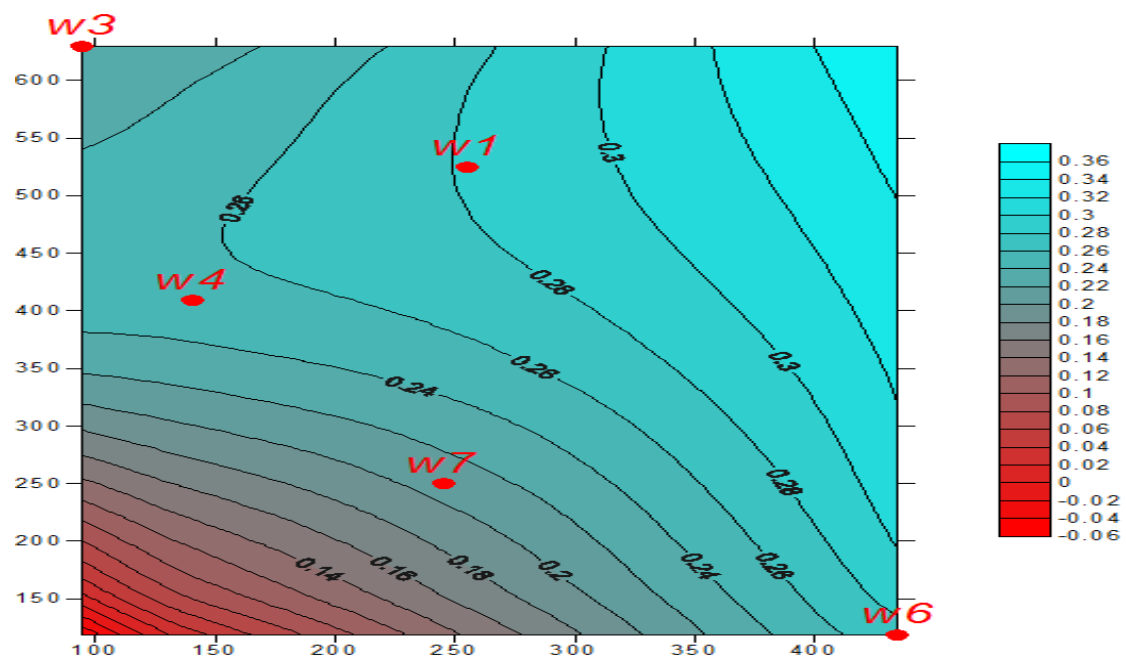


Figure (4-1) this map explain the effective porosity distribution for Aradeiba formation in bamboo field.

4.2. Permeability

There are several methods to determine permeability, the accurate method coring. We estimate the permeability distribution for Aradeiba formation at bamboo field using coring method.

Coring data:

Ten samples were taken from the layer Aradeiba of five wells from depth (1250 to 1287) meters and although it is not the subject of study within the wells, but in the same field and the same layer and based on that samples are taken for the same layer have been adopted for the rest of the wells.

Plot the porosity versus permeability where porosity at X-axis and permeability at Y-axis:

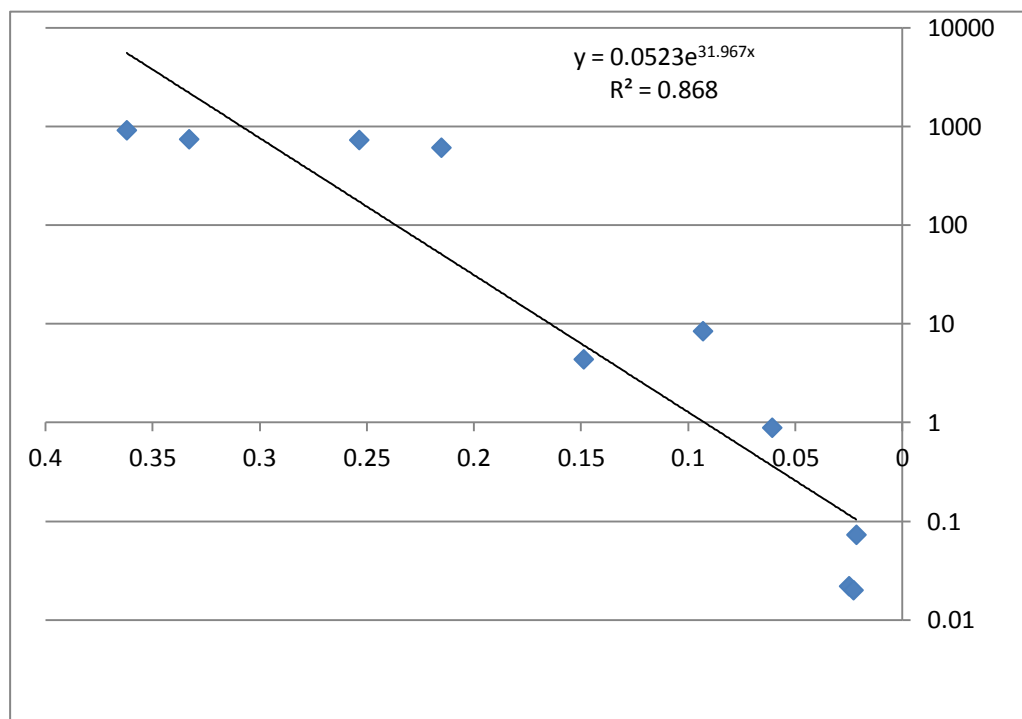


Figure (4-2): porosity versus permeability from coring data

This equation below extracted from the plot above to determine the permeability for Aradeiba formation by substitute the effective porosity value in the equation and the result will be the permeability.

$$Y=0.052e^{(31.96*X)} \dots (4-6)$$

Where:

Y=Permeability.

X=Effective porosity.

The tables below (4-16) , (4-17) , (4-18) , (4-19) , (4-20) explain the permeability calculated from coring data:

Table (4-16): Permeability for Well 1:

Sand Zone	Depth M	ϕ_e	Permeability Md
1	915 – 1020.45	0.292	86.49
2	1023.45 – 1054.8	0.317	57.166
3	1068.8 – 1070.4	0.216	3372.7
4	1072.05 – 1074.45	0.225	16440.06

Table (4-17): Permeability for Well 3:

sand Zone	Depth M	ϕ_e	Permeability md
1	932 – 1072.6	0.282	82.47
2	1090 – 1096.8	0.219	92970.45
3	1099- 1107.5	0.205	867.72
4	1119.5 – 1123	0.216	929.97
5	1134.5 – 1186.4	0.272	267.85
6	1196.8 – 1197.89	0.264	9510.69
7	1200 – 1202.6	0.295	103.21
8	1219.4 – 1245.7	0.244	155.36
9	1247.7 – 1261.3	0.336	638.87
10	1263.5 – 1266	0.16	1804.75

Table (4-18): Permeability for Well 4:

Sand Zone	Depth M	ϕ_e	Permeability Md
1	897.03 – 937.87	0.311	10672.3
2	948 – 972.92	0.306	3983.4
3	942.07 – 989.99	0.238	140
4	1032.1 – 1063	0.252	749
5	1088.3 – 1098.1	0.169	96.6
6	1211.1 – 1220	0.332	5113.4
7	1251.1 – 1253.9	0.078	13.5

Table (4-19): Permeability for Well 6:

Sand Zone	Depth M	ϕ_e	Permeability md
1	900.07 – 904.95	0.352	2387.34
2	911.05 – 920.95	0.228	936.54
3	991.06 – 998.98	0.293	2772.63
4	1009 – 1019.9	0.293	2960.14
5	1034 – 1248	0.248	18681.52

Table (4-20): Permeability for Well 7:

Sand Zone	Depth M	ϕ_e	Permeability md
1	867 – 981.91	0.272	860.66
2	990.4 – 1058.9	0.277	6040.43
3	1081.1 – 1097.9	0.147	27.42
4	1133.1 – 1140.9	0.287	7479.23
5	1144 – 1154.9	0.339	40490.1
6	1205 – 1229.9	0.327	11397.52
7	1261.1 – 1266.9	0.087	19.138

By using **surfur8 software** the permeability from the equation above used to extract contour map which illustrate the permeability distribution for Aradeiba formation in bamboo field for the five wells show in figure (4-3) below.

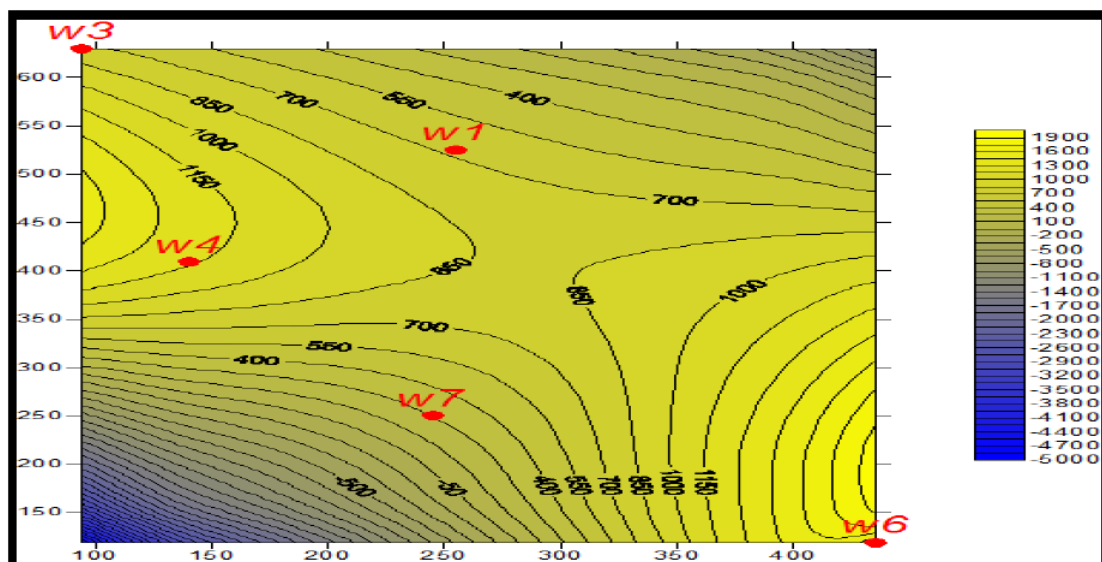


Figure (4-3): explain permeability distribution for Aradeiba formation in bamboo field

4.3. Saturation:

The saturation was determined by two methods and makes a comparison between them.

The first method by Archie equation:

$$S_w = \sqrt[n]{\frac{a \cdot R_w}{R_t \cdot \phi^m}} \dots (4-7)$$

M = Cementation factor

N = Saturation exponent

A = Tortuosity factor

S_w = Effective water saturation

R_w = Formation water resistivity

R_t = Input resistivity curve

The second method by Indonesian method from IP software. The tables below (4-21) , (4-22) , (4-23) , (4-24) , (4-25) explain the saturation by Archie equation and by Indonesian method:

Table (4-21): Saturation for Well 1:

Sand zone	Depth	Sw(Archie)	Sw(Indonesian)
1	915 – 1020.45	0.997	0.999
2	1023.45 – 1054.8	1	1
3	1068.8 – 1070.4	0.899	0.892
4	1072.05 – 1074.45	0.896	0.895

Table (4-22): Saturation for Well 3:

Sand zone	Depth	Sw(Archie)	Sw(Indonesian)
1	932 – 1072.6	0.987	0.988
2	1090 – 1096.8	0.993	0.992
3	1099- 1107.5	0.888	0.889
4	1119.5 – 1123	0.997	0.996
5	1134.5 – 1186.4	1	1
6	1196.8 – 1197.89	1	1
7	1200 – 1202.6	1	1
8	1219.4 – 1245.7	0.998	0.999
9	1247.7 – 1261.3	0.993	0.992
10	1263.5 – 1266	0.65	0.65

Table (4-23): Saturation for Well 4:

Sand zone	Depth	Sw(Archie)	Sw(Indonesian)
1	897.03 – 937.87	0.997	0.974
2	948 – 972.92	0.994	0.992
3	942.07 – 989.99	1	1
4	1032.1 – 1063	0.941	0.937
5	1088.3 – 1098.1	0.573	0.566
6	1211.1 – 1220	0.999	0.997
7	1251.1 – 1253.9	0.441	0.422

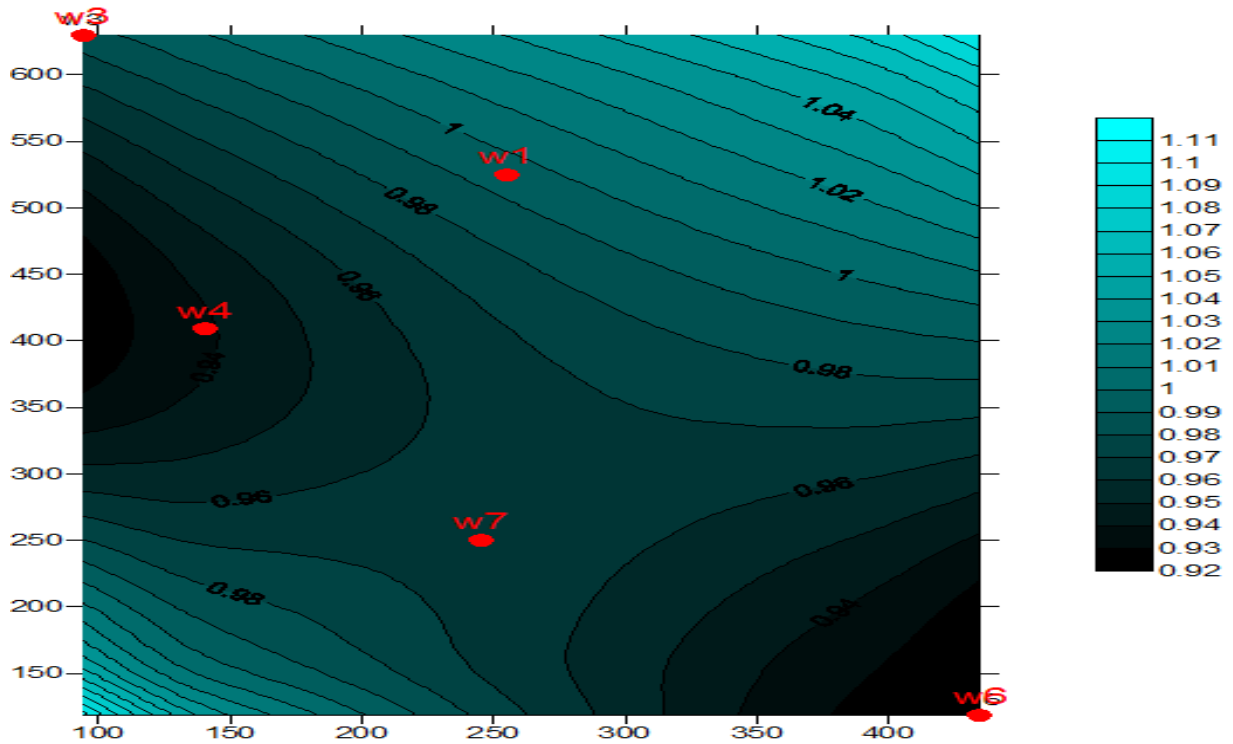
Table (4-24): Saturation for Well 6:

Sand zone	Depth	Sw(Archie)	Sw(Indonesian)
1	900.07 – 904.95	0.992	0.993
2	911.05 – 920.95	1	1
3	991.06 – 998.98	1	1
4	1009 – 1019.9	1	1
5	1034 – 1248	0.93	0.932

Table (4-25): Saturation for Well 7:

Sand zone	Depth	Sw(Archie)	Sw(Indonesian)
1	867 – 981.91	0.994	0.994
2	990.4 – 1058.9	0.977	0.977
3	1081.1 – 1097.9	0.864	0.864
4	1133.1 – 1140.9	1	1
5	1144 – 1154.9	0.968	0.969
6	1205 – 1229.9	0.971	0.972
7	1261.1 – 1266.9	0.462	0.462

By using surfur8 software the Saturation data by Archie equation used to extract contour map which illustrate the saturation distribution by Archie equation for Aradeiba formation in bamboo field for the five wells show in figure (4-4) below.



Figure(4-4): Explain Saturation distribution by Archie equation for Aradeiba formation in bamboo field

4.4. Pore pressure

4.4.1. Numerical Methodology for Pressure Estimation:

The accurate prediction of pore pressure and fracture gradients has become almost essential to the drilling of shallow and deep wells with higher than normal pore pressures. Costs and drilling problems can be reduced substantially by the early recognition of abnormally high pore pressure.

In this study, as mentioned in Chapter 3 the study is focusing on utilize wire-line logging data primarily using sonic reading from conventional composite logs in five different wells located at Bamboo west field. Those wells are spread / distributed across the field to represent the pore pressure pattern or profile within this area. The first well BAW-01 located at the right side of the area of study , the second well BAW-03 is at the top of the field (North West of bamboo west field), the third well BAW-04 is located at the left side of the area of study , the fourth well BAW-06 is located at the bottom of the area of study (South East of bamboo west field), and the last well BAW-07 in the middle.

The base of the calculation depends on a relationship between pressure, density and depth:

$$P = \rho * g * h \dots (4-8)$$

Where:

g: Gravity acceleration (m/s²).

4.4.2. Pressure Numerical Estimation:

All available data of 5 wells were collected, those data include the following:

- 1- Sonic (Δt) transient time readings in $\mu\text{s}/\text{ft}$.
- 2- Bulk Density (RHOB) readings in g/cc.

One method was used for formation pore pressure prediction; treating data of all wells as one single group to estimate pressure in Aradeiba formation.

The base of this work as mentioned previously is to build an equation to estimate pressure based on some log data as explained in figure (4-5). Only one correlation will be created, based on sonic data.

In order to create sonic –based equation, density (ρ) must be a function of sonic, this is achieved by plotting bulk density with log data; as for depth, same as density it must be a function of sonic as well thus by plotting depth versus sonic.

To obtain the target of this work, the method was utilized to come out with the most reliable equations. This method used to deal with the data of all five wells as a single well and do the calculation once to get an equation for pore pressure estimation for Aradeiba formation.

4.4.3. Pore pressure Estimation Method:

After plotting wells BAW – 01, 03,04,06,07 sonic data against bulk density results were found as in figures (4-5) and (4-6) below:

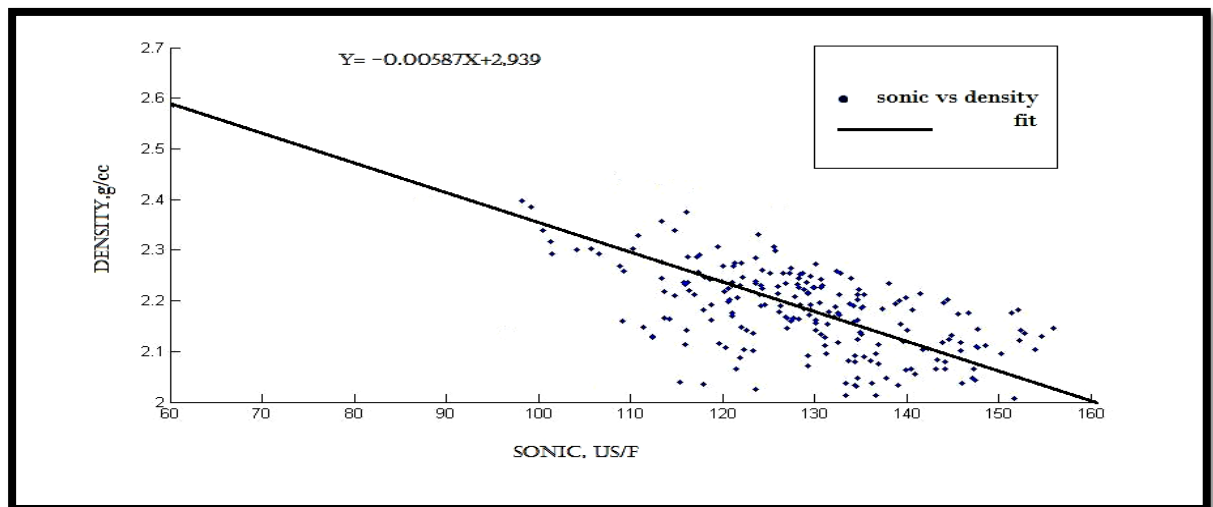


Figure (4-5): Sonic vs Density

From the above figures Bulk density – Sonic equation is:

$$Y = -0.00587X + 2.939 \dots (4-9)$$

Next figures showing the plot of sonic data for selected wells against their depth and results are shown as in figures below:

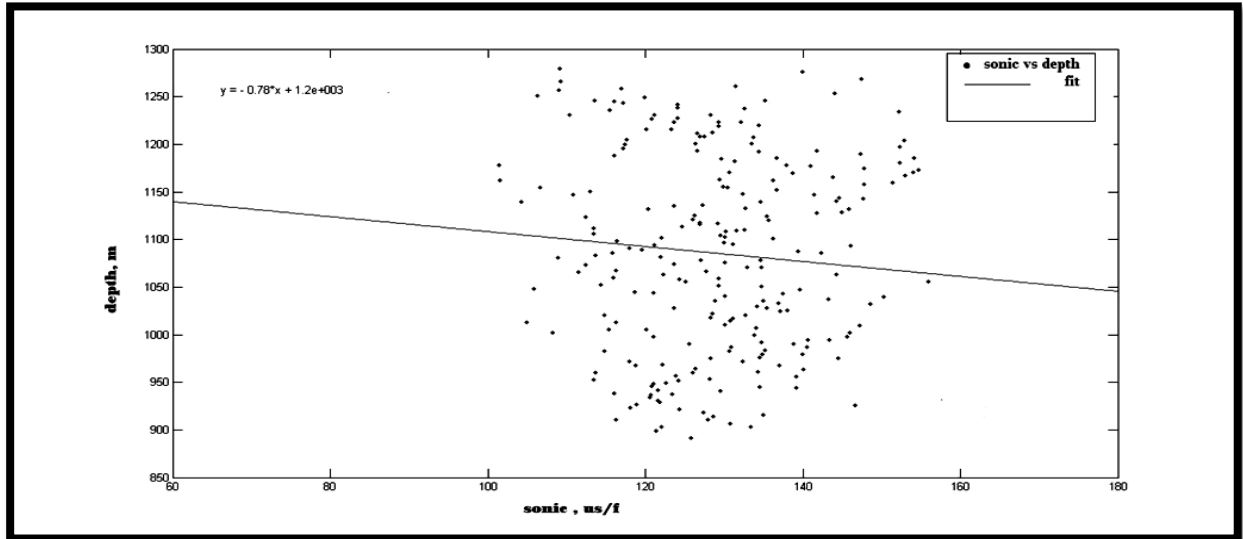


Figure (4-6): Sonic versus Depth

Depth – sonic equation is:

$$Y = -0.78X + 1200 \dots (4-10)$$

Pressure is estimated by using above equation, therefore the pore pressure equation for Aradeiba formation is expressed as

$$P = 0.0031X^2 - 6.8579X + 3299.724 \dots (4-11)$$

The result where plotted against depth to give the pressure profile for Aradeiba formation using sonic data

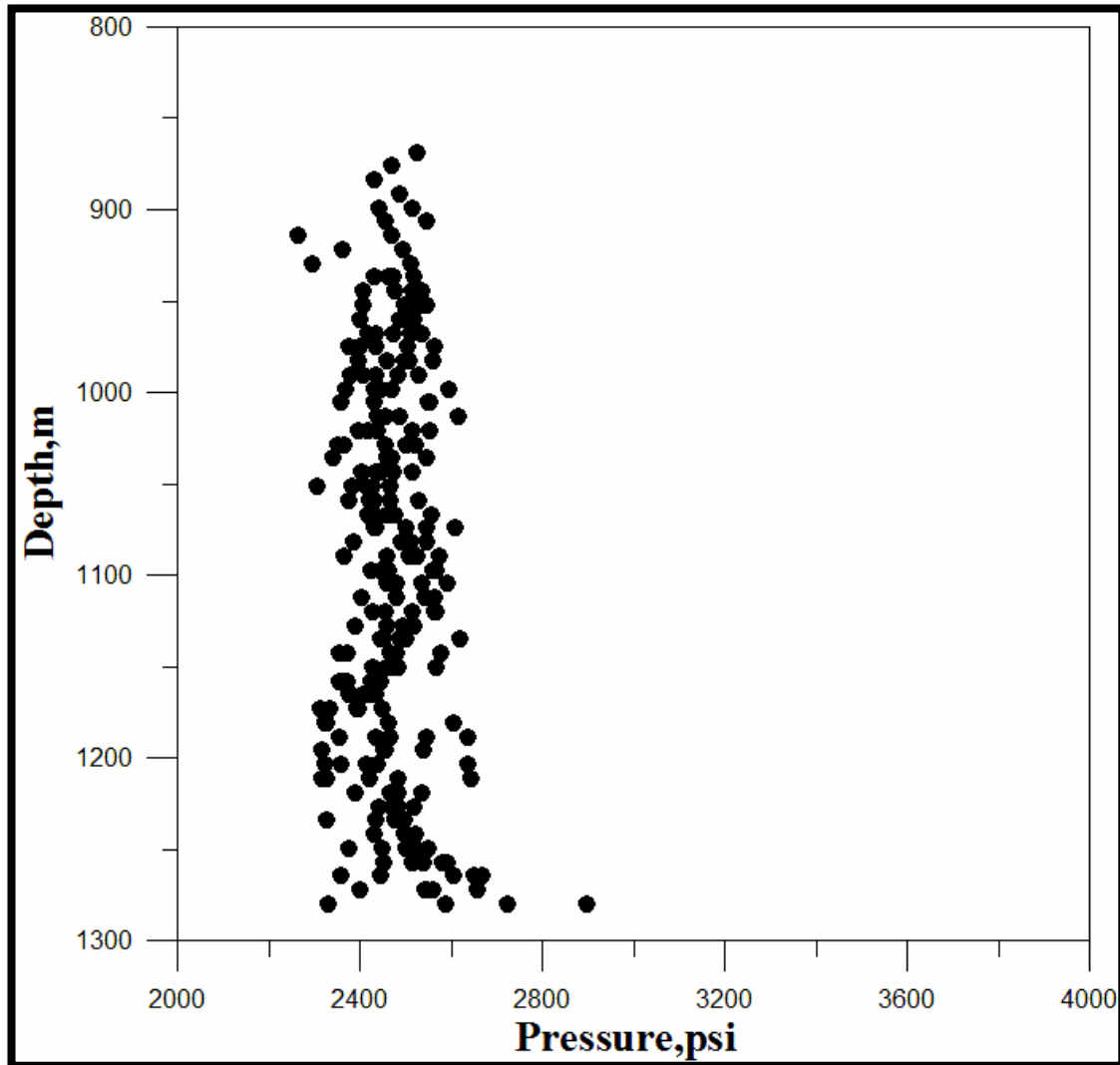


Figure (4-7): Pressure calculated versus depth

Finally, comparison for pore pressure distribution in Aradeiba formation represented by contour lines was constructed by surfer software as in figure (4-8) below. This comparison involves pressure results from the sonic method. Figure (4-6) plotted using surfer software, showing that the pressure distribution for calculated pressure in sonic log.

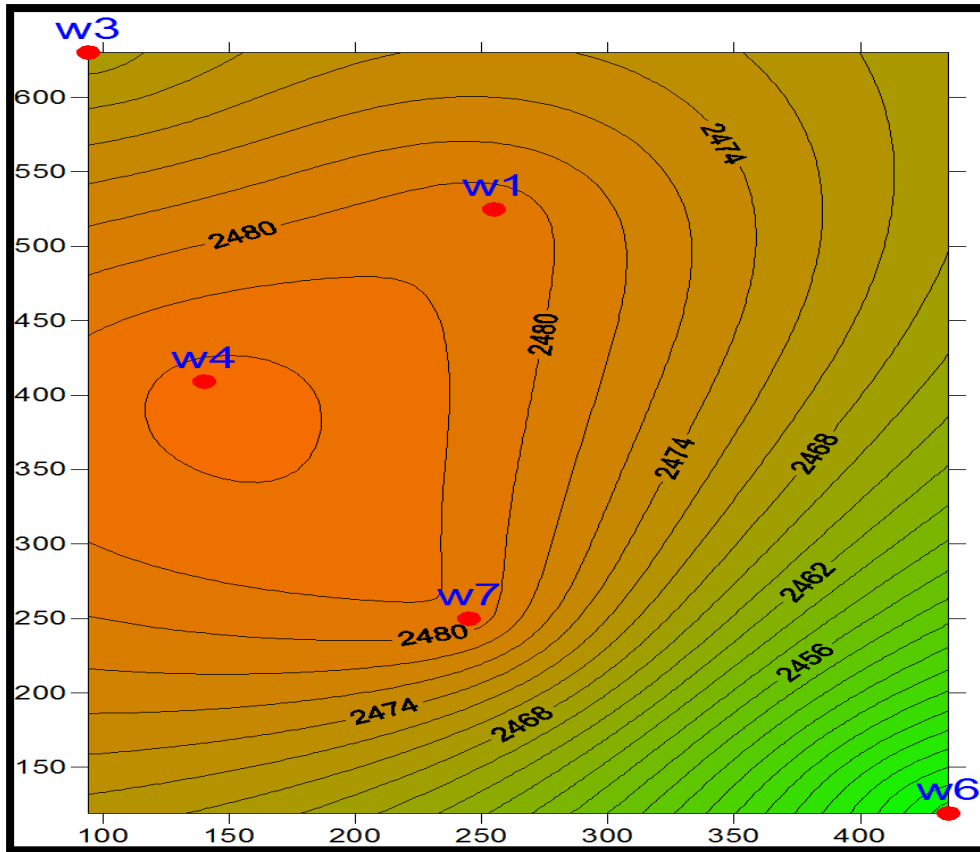


Figure (4-8): Explain Pressure estimated distribution for Aradeiba formation using sonic equation.

Chapter 5

RESULT & DISCUSSION

Chapter 5

RESULT AND DISCUSION

For previous accounts have reached the results illustrate the distribution of characteristics in the Aradeiba layer , and this section will discuss these result that they expose to it in the form of contour maps to illustrate the distribution of these properties and best drilling location .

- The water saturation is extremely high $S_w = 0.9$ Figure (5-1)
- From the Porosity map, it's have a good range; however a good porosity range from 20 to 32 Figure(5-2).
- The permeability has a good value also; above 400 the permeability considered fine. Figure(5-3).
- The pressure gradient map will help the drilling engineer to control the well; and it will be with great benefit if compared with the Depth structure map Figure(5-4).
- From the plotting of the pressure VS depth, it has been seen that the pressure range from 2200-2800 psi in reservoir thickness around 500m Figure(5-5).
- From the water saturation by Arch equation and by Indonesian(IP) plotting the reservoir considers as shallow water pouring reservoir with 100% water saturation; the possibility to find any oil accumulation will be impossible Figure(5-6).
- From the permeability plotting the permeability range from 10-100MD which was very good Figure(5-7).
- From the porosity plotting; the porosity range from 0.2-0.4 which was a very good Figure(5-8).
- In a proper discussion for the maps it should start by the porosity, permeability, water saturation and pressure gradient.
- The NE part has a high porosity but have a low permeability and high water saturation Figure(5-1),(5-2),(5-3).
- The NW part has a high permeability but have a moderate porosity and high water saturation Figure(5-1),(5-2),(5-3).

- The SW part has a relatively low water saturation; but that probably due to low porosity consequently with low permeability Figure(5-1),(5-2),(5-3).
- The SE part has low water saturation in addition to good porosity, & in the company of excellent permeability range. Figure(5-1),(5-2),(5-3).
- The central west has low water saturation and good porosity along with good permeability Figure(5-1),(5-2),(5-3).
- If we take a look to the tow maps permeability and water saturation we will find that there are two compartments on the trend of the contours and to explain that we need to see the structure map of the reservoir. Figure(5-1),(5-3).
- The two possible locations are: 1/ on the central west 0.96-0.92. 2/ on the SE 0.96-0.92 on the water saturation map. Figure(5-1).
- So we have two locations with good probability. The SE and the Central W prospects between W7 & W6 and around W4. Figure(5-9).
- The Pressure gradient map will play a very important roll to rank our proposed prospects wells in term of production. Figure(5-4).
- Because SE prospect (between W7 & W6) has low pressure gradient will be ranking No. 2; and prospect Central W (around W4) has high pressure gradient will be ranking No. 1. Figure(5-4).
- Finally we have a prospect well location west W4 between the contours 0.96-0.90 on the water saturation map. Figure(5-1).

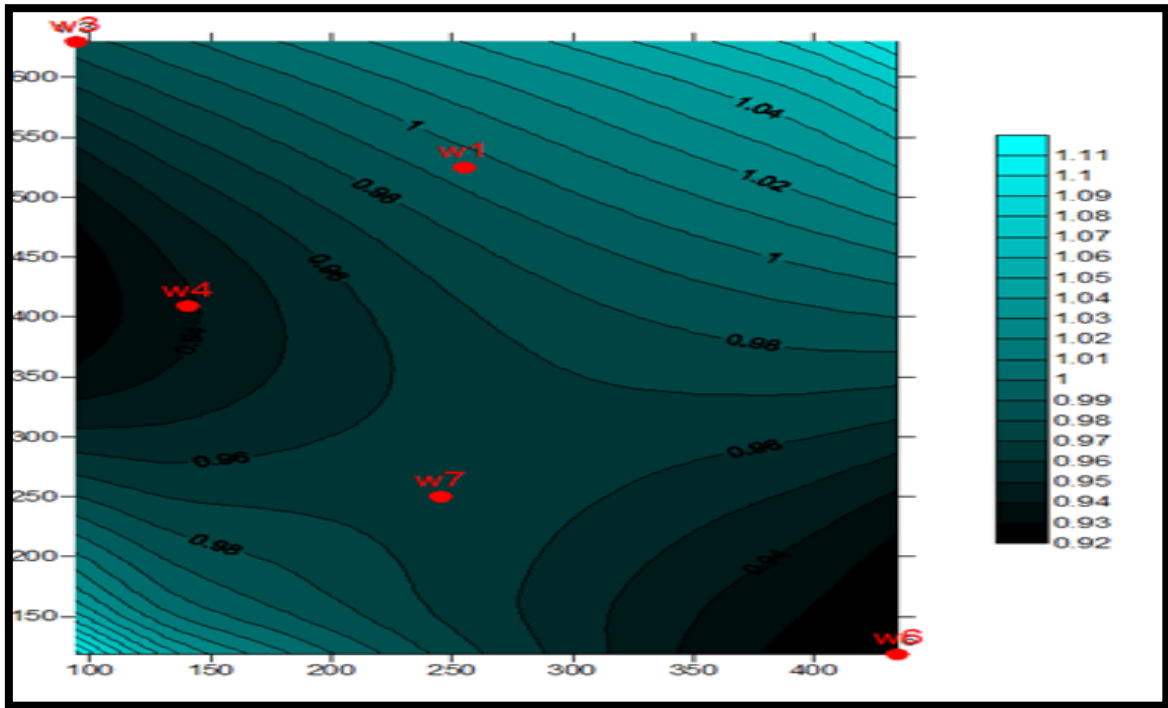
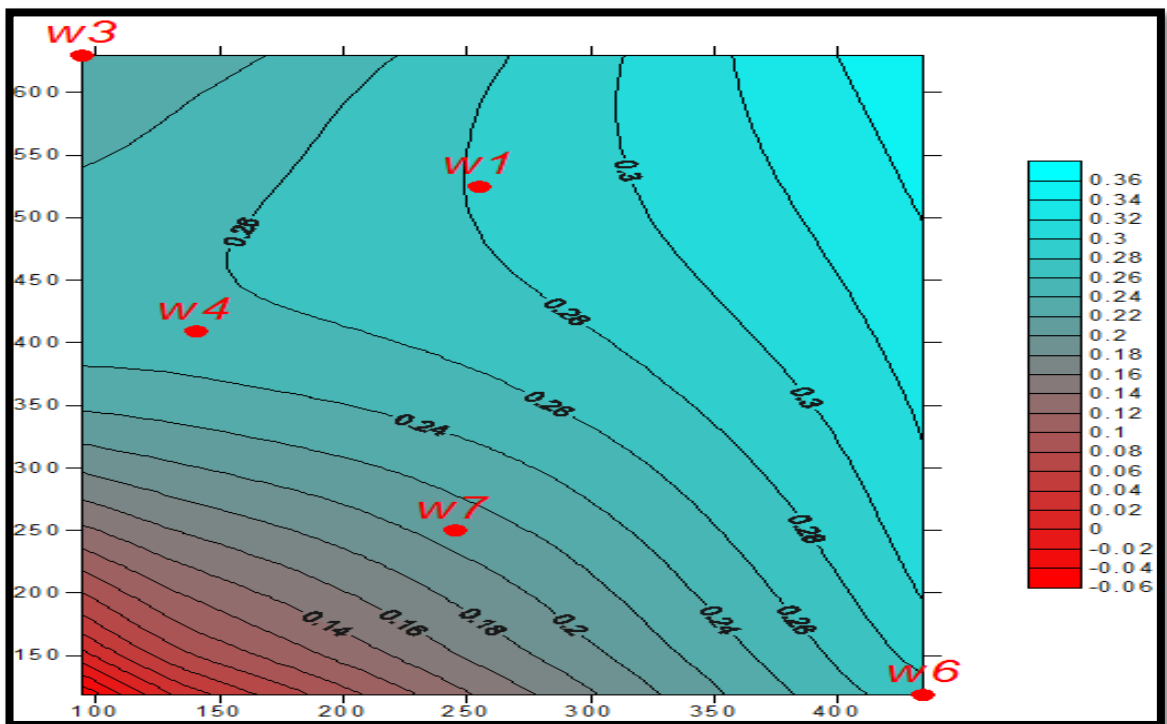
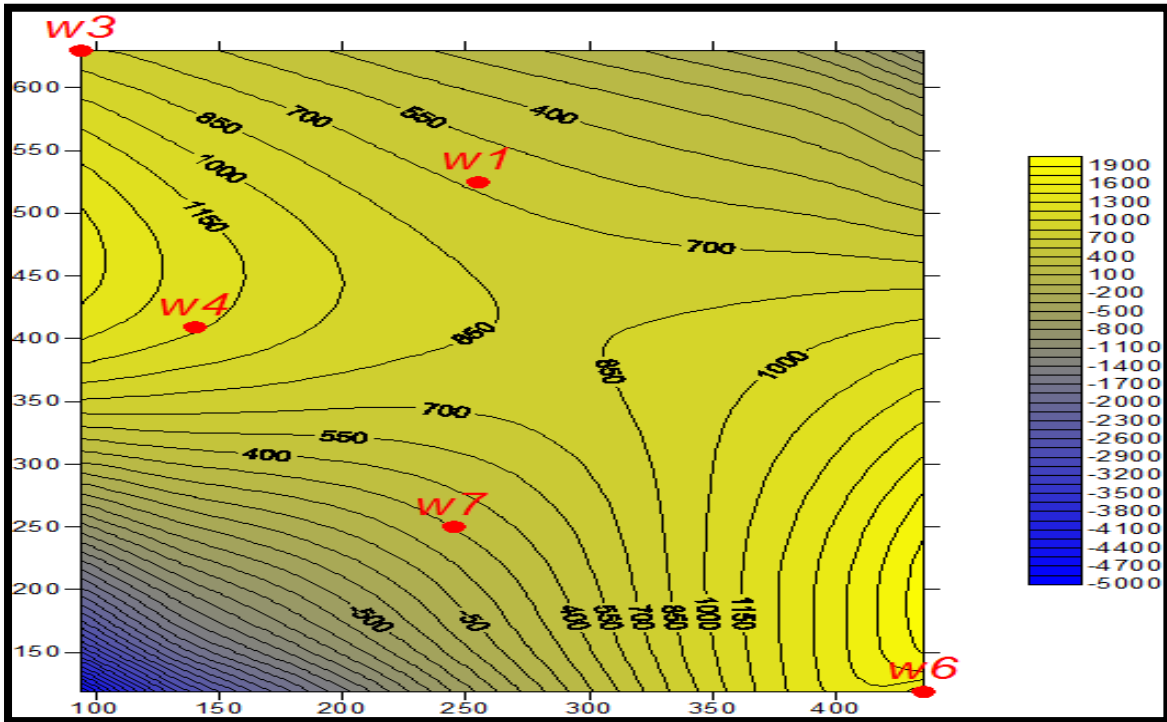


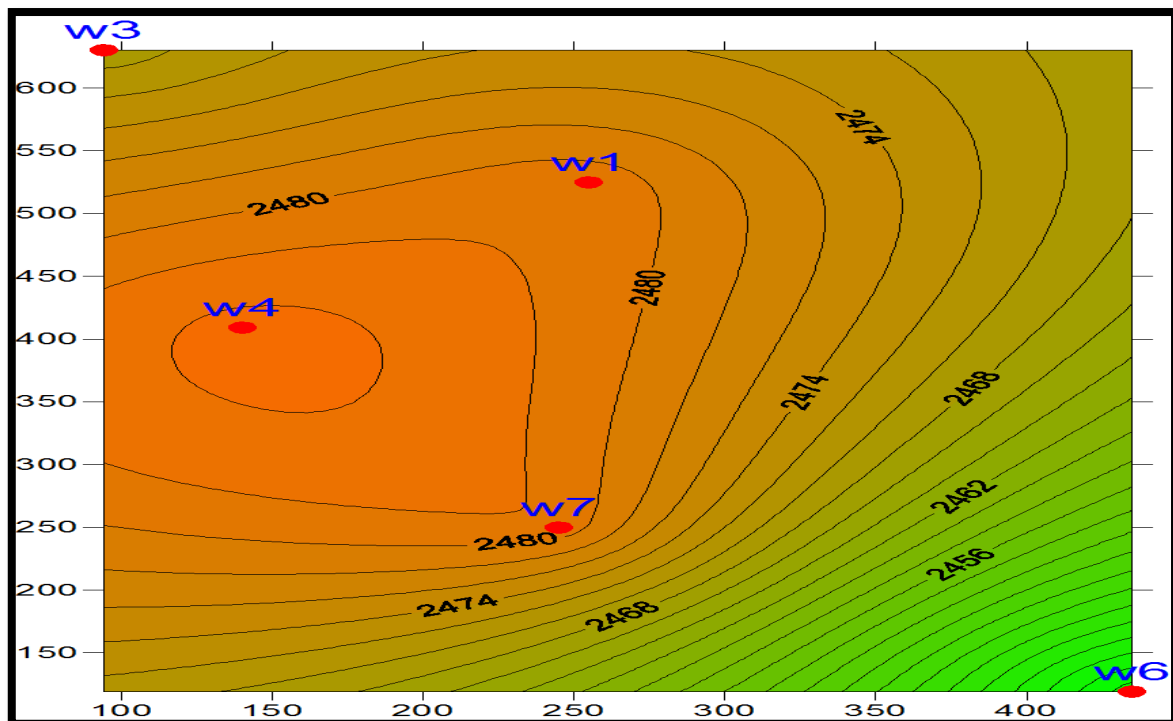
Figure (5-1): saturation contour map



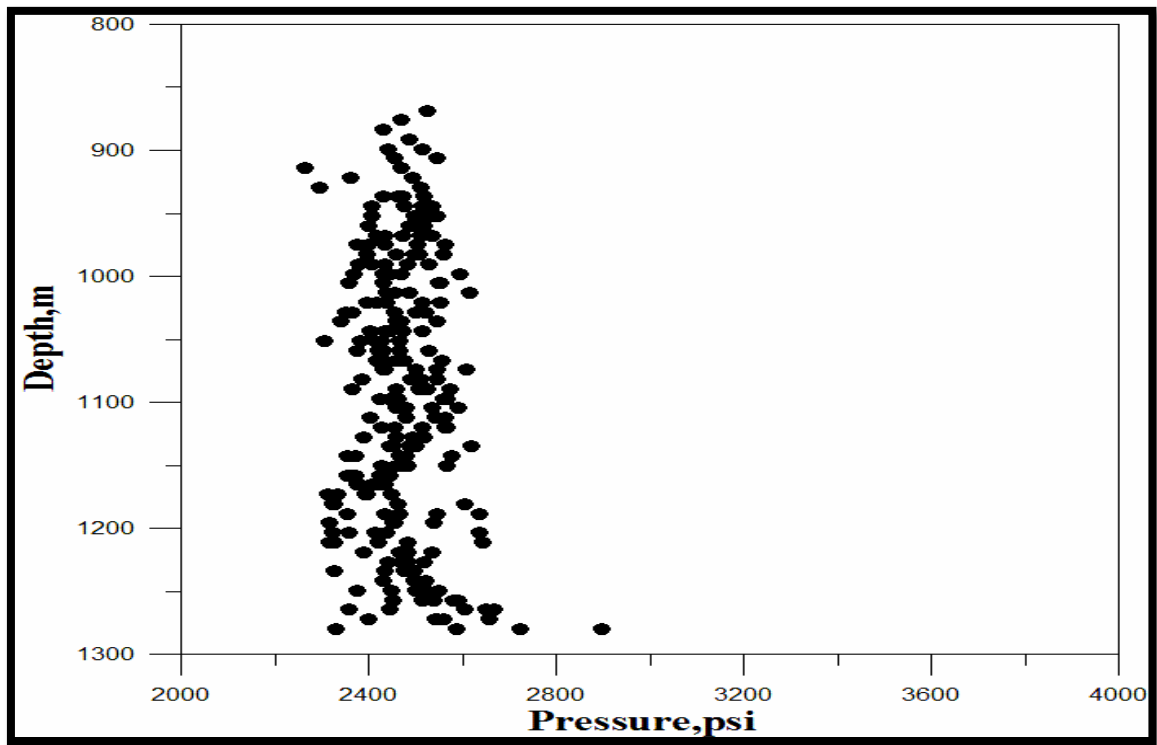
Figure(5-2): effective porosity contour map



Figure(5-3): permeability contour map

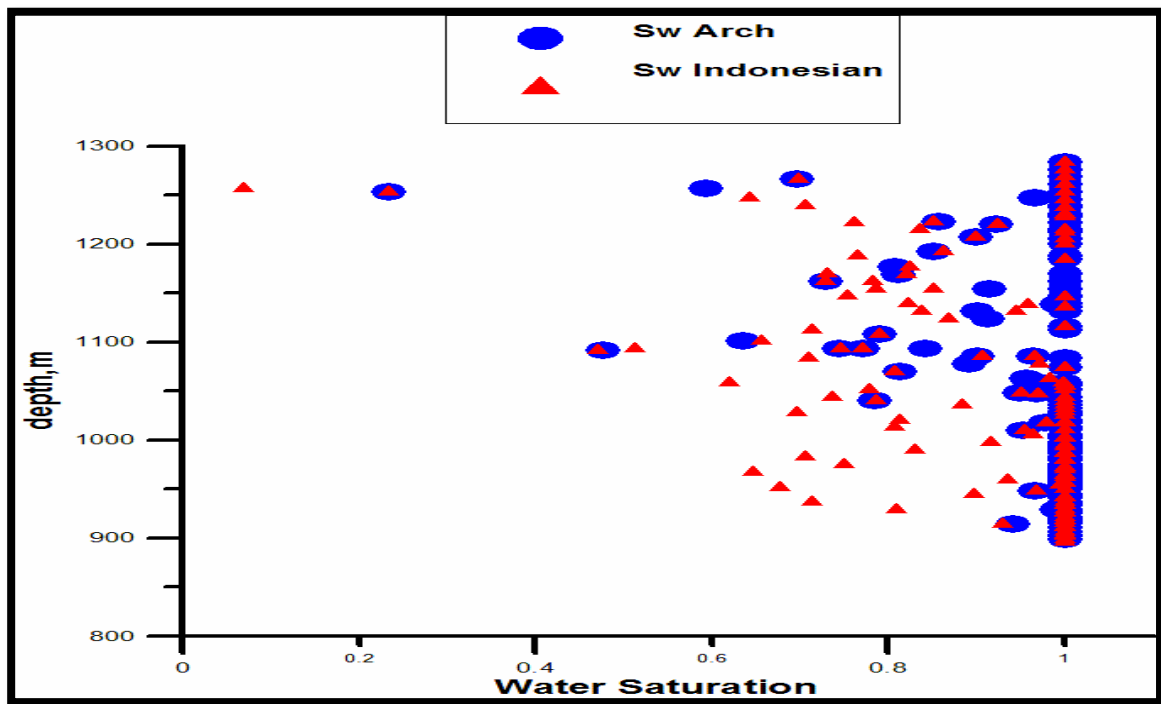


Figure(5-4): pressure contour map



Figure(5-5) plot Pressure VS Depth

comparing with IP:



Figure(5-6) plot Saturation by Arch equation and by Indonesian(IP) VS Depth

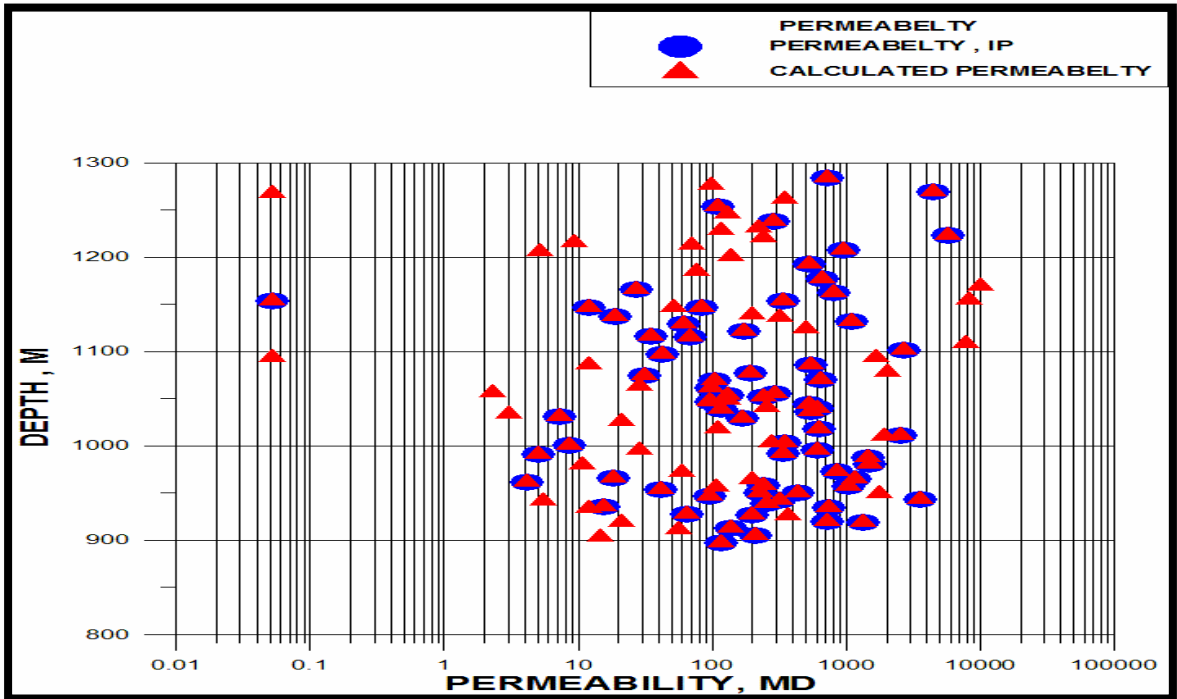


Figure (5-7) plot calculated permeability and permeability by IP VS Depth

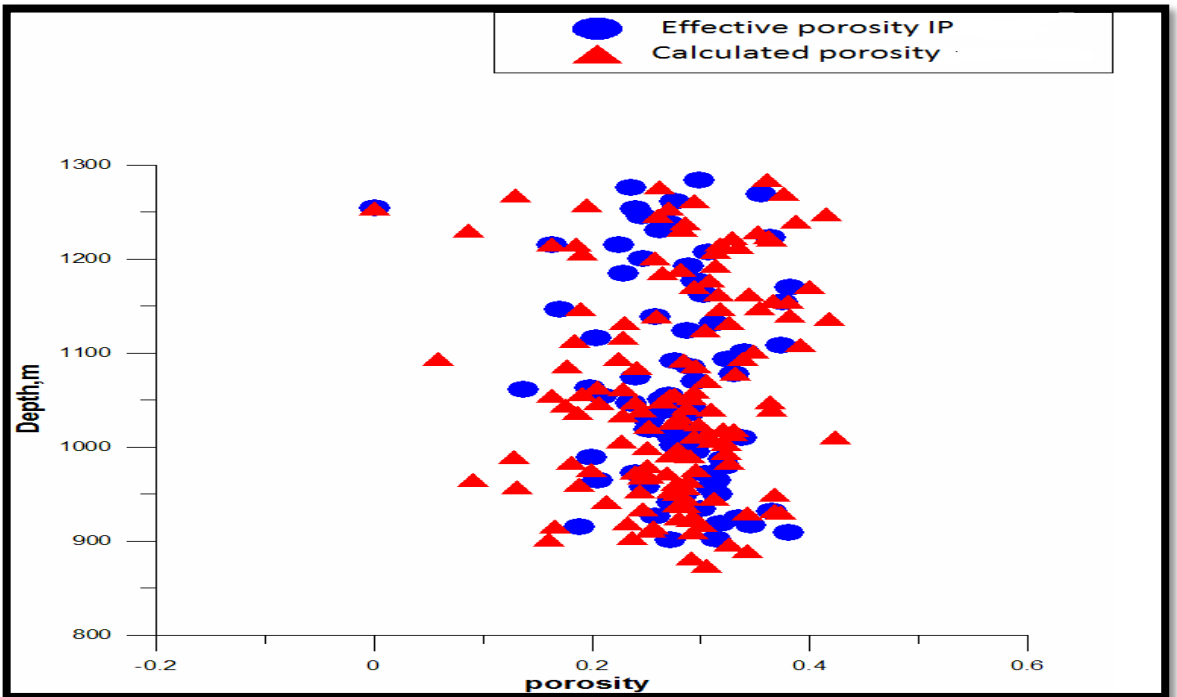


Figure (5-8) plot calculated porosity and porosity by IP VS Depth

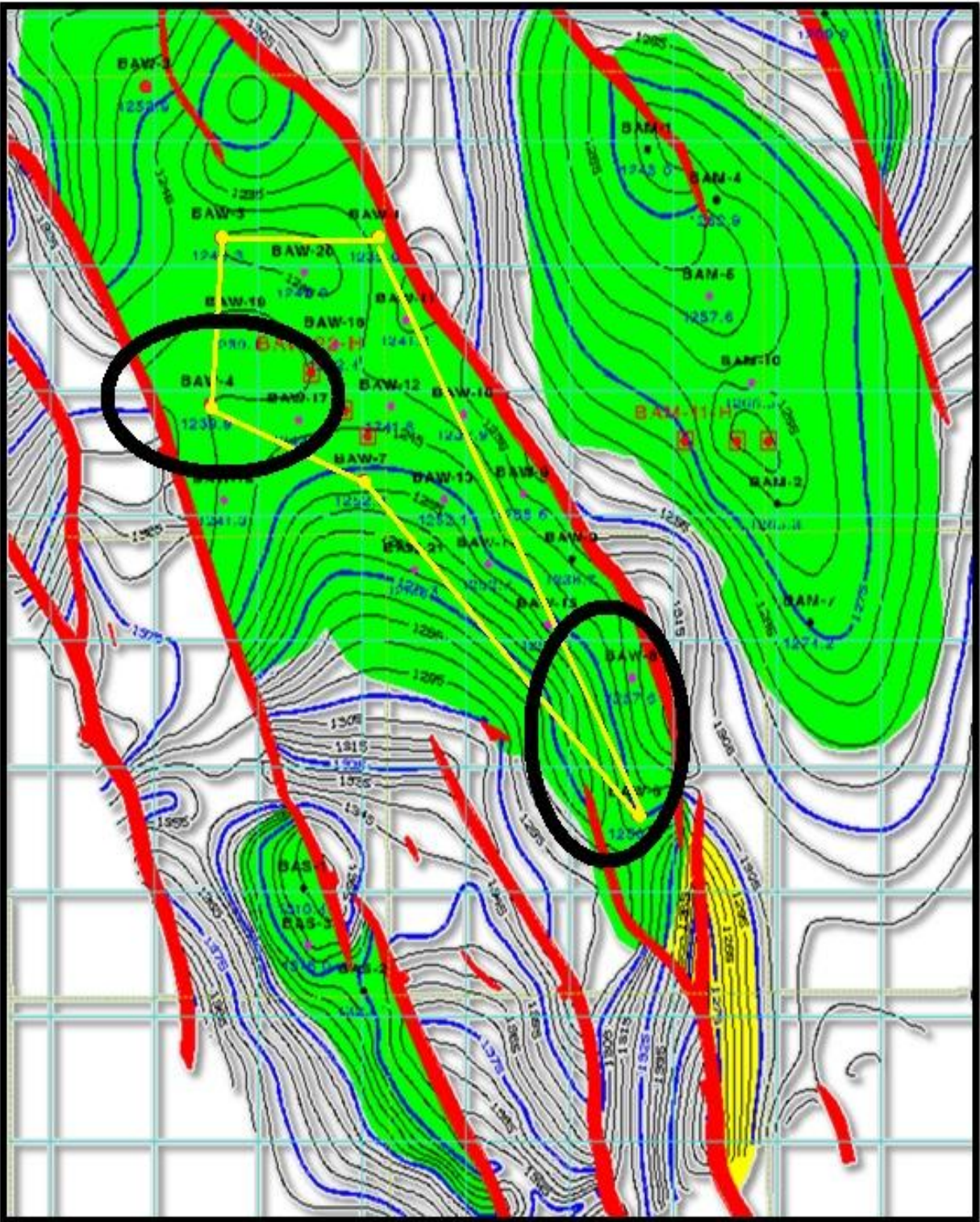


Figure (4-9) locations with good probability

Conclusion and Recommendation

Conclusion :

The new in this project is the attention of these properties calculated (porosity, permeability, saturation and pressure) at the field level and not at the level of the wells only, depending on the data set of wells we can expect the distribution of these properties through the field (Area straitened between wells) to determine the direction of increase and decrease (gradient) of these physical properties.

Finally from the evaluation of Aradeiba formation of bamboo field by calculating the physical properties (porosity, permeability ,saturation and pressure) by using logging data , we think more researches must be focusing in physical properties of formation to give certain overview to the future decision will be taken.

Also is this research has included the evaluation of the formation entirely ? Of course not, therefore advise those who come after us to study the area that starts from the point where we stood then.

Results of the study were to come to know the distribution of properties of the layer in the field, where he found that the values of effective porosity in the layer was good and ranged between (20-32%) and good distribution and increase as we head east. As for the permeability values, find that in a good layer and higher than 400 MD, but distributed irregularly in the layer where the field than on the outskirts of east and west. As for the saturation and found that the high value of up to almost 100%, which reduces the chances of the presence of hydrocarbons in the layer and that is the greatest probability of the presence of water . Pressure was found to be distributed in layer was gradual and regular and appropriate as comparing the experimental method was found in the range of 2200-2400 psi .

layer can be considered as a good reservoir porosity and permeability values and distributed in the field, but in view of the values of saturation found that the layer containing quantities of oil in and it's not economically feasible.

Recommendation:

After studying the results obtained, we find that there are a few recommendations:

- 1 – Don't production from this formation in spite of it oil contain , but it is not economically feasible.
- 2 –Give more attention to physical properties calculated in the search field on the level and not only at the level of the well, which helps in the development of the field and make the most of it.
- 3 – Design a software to calculate these properties, including the work of the contour map showing the distribution of properties in the field.

References :

Abhijit Y . Dandekar , Petroleum Reservoir and fluid properties , 2006 ,Boca Raton , London, UK.

Ayah Abdelahi Fadlallah , Estimate of pressure Regime – Bantiu MSc 1 , 2012 , SUST .

Browne, S. E. and J. D. Fairhead (1983). Gravity study of the Central African rift system: a model of continental disruption; 1, the Ngaoundere and Abu Gabra rifts, in P. Morgan, ed., Processes of continental rifting: Tectonophysics,

Craft . C.B and Hwkins . M.F , Applied Petroleum Reservoir Engineering , Reviewed by Roland E . Terry , 1991, Prentice Hall , upper saddle river , NJ 07458

Fairhead, J. D. (1988). Mesozoic plate tectonic reconstructions of the central South Atlantic Ocean: the role of the West and Central African rift system. Tectonophysics

. Giedt, Norman, R., 1990, Unity field—Sudan Muglad rift basin, Upper Nile province, inAAPG Treatise in Petroleum Geology, Structural traps III: Tectonic fold and fault traps

Glover. P , Petrophysics MSc Corse Note , 2001, un publish.

James W . Amyx and Daniel M . Bass , Robert L .Whiting , Petroleum Reservoir Engineering , 1988 , Mc Grew – Hill , USA.

Kaska, H.V., 1989. A spore and pollen zonation of the Early Cretaceous to Tertiary non-marine sediments of central Sudan. Palynology

Leblond . A , Basics of reservoir Engineering , Translated by Legisement . R.Cosse, 1993, Editions Technip , Paris , France

Mahapatra . G . B , Text book physical geology , 1994, Dary Ganj , New Delhi , India.

Rabia.H , Well Engineering and Construction , 2001 , Entrac Consulting , UK.

Roy . J . P , Essentials of Reservoir Engineering , 2007 , Editions Technip , Paris , printed in France.

Schull, T.J., 1988. Rift basins of interior Sudan. Petroleum exploration and discovery. American Association Petroleum Geologists Bulletin

Shams Alflah Ahmed Ali Bilola , Application of Rock Stability and Drilling Mud Selection Using Mohrin In Bamboo Wester Field – Sudan MSc , 2009, SUST.

Vail, J.R., 1978. Outline of the geological and mineral deposits of the Democratic Republic of the Sudan and adjacent areas. Overseas Geology and Mineral Resources

Appendix

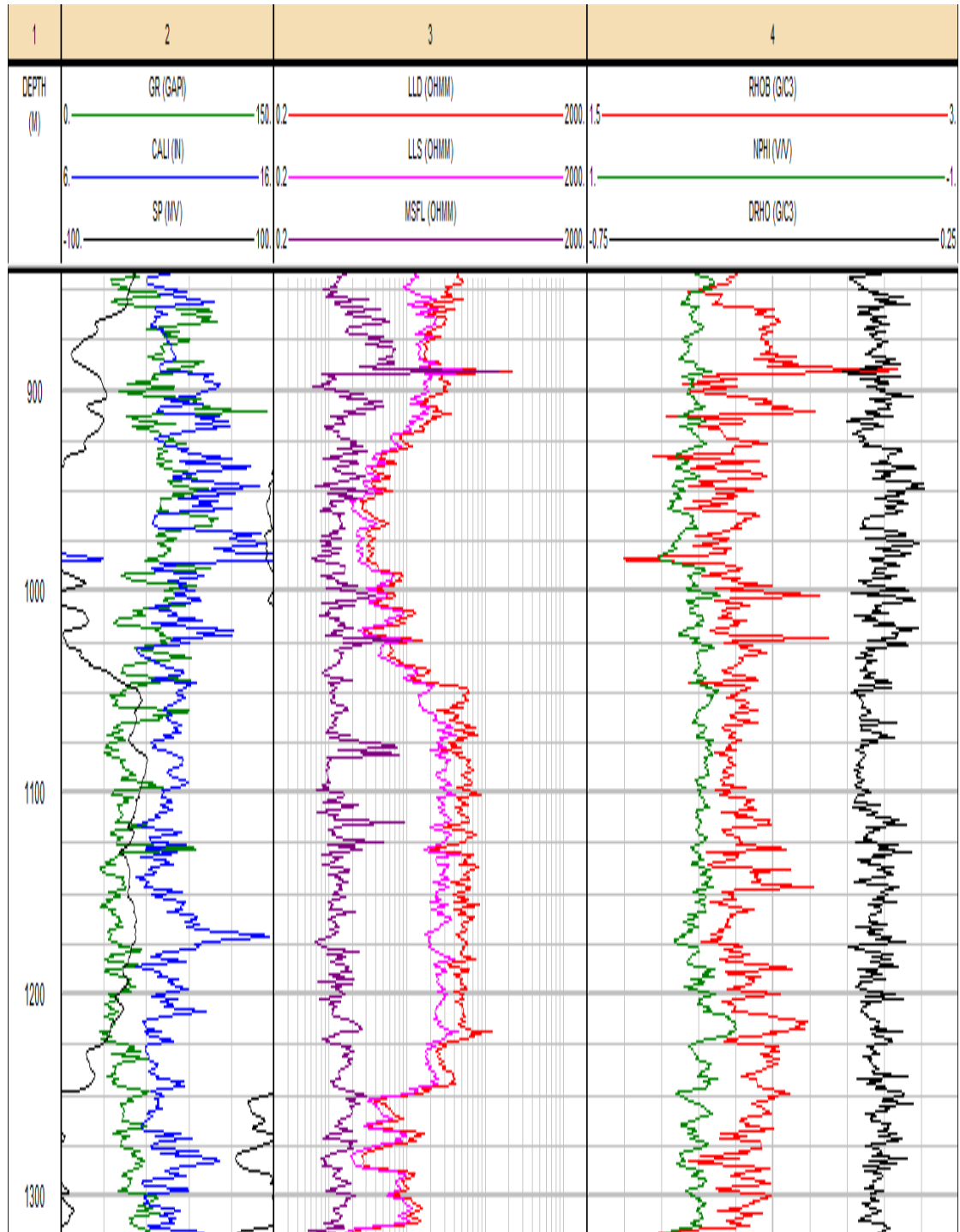


Figure 1: Log Data

**AIR-BRINE CAPILLARY PRESSURE
BY POROUS PLATE METHOD**

TABLE : 3.1

COMPANY : GNPOC

WELL : BAMBOO WEST-5

JOB NO. : C35100

Sample No.	Depth (meter)	Ka (mD)	Porosity (%)	Brine Saturation (% Pore Space)						
				1*	4	10	30	60	100	200
1	1250.58	8.45	9.3	92.0	82.7	76.3	70.0	66.2	64.2	62.5
2	1253.15	4.38	14.9	94.3	83.1	77.4	71.6	67.9	65.7	64.2
3	1254.40	0.02	2.5	98.7	93.0	86.4	79.1	74.9	72.9	69.9
4	1256.38	0.89	6.1	86.5	83.5	80.9	75.6	71.2	68.4	66.6
5	1259.44	744	33.3	40.6	31.2	24.3	21.0	20.0	19.4	19.1
6	1272.49	0.07	2.1	98.1	90.3	83.9	76.9	72.0	70.0	68.0
7	1273.10	0.02	2.3	90.4	87.2	83.5	77.6	73.3	70.8	69.0
8	1285.67	611	21.5	43.9	27.9	19.4	16.3	15.0	14.9	14.8
9	1286.61	917	36.2	39.1	28.3	19.6	17.2	16.3	16.0	16.1
10	1287.71	731	25.4	40.0	25.9	18.7	15.6	14.7	14.5	14.5

* : Capillary Pressure (Psig)

Ka : Air Permeability (millidarcies)

Figure 2: Coring Data

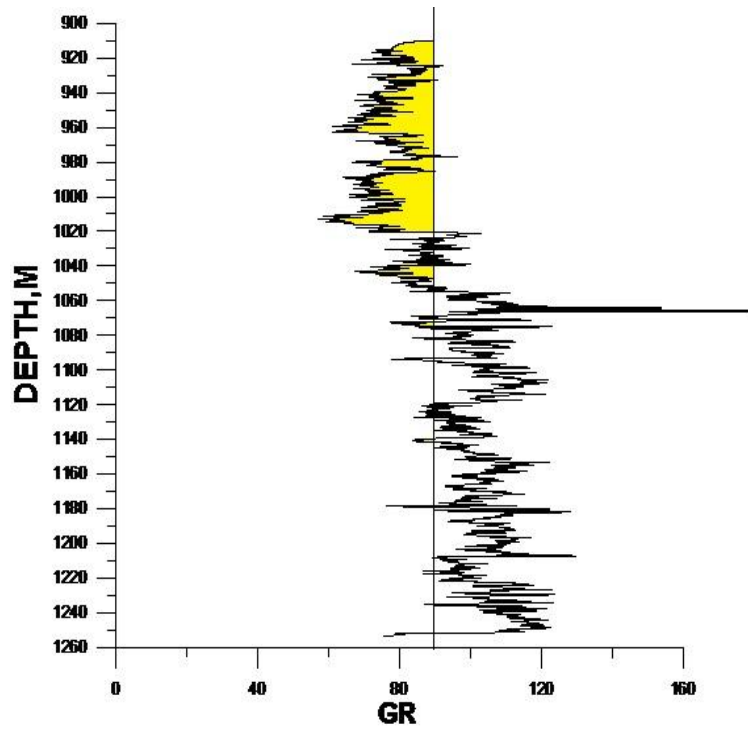


Figure 3: Gama Ray For Well 1

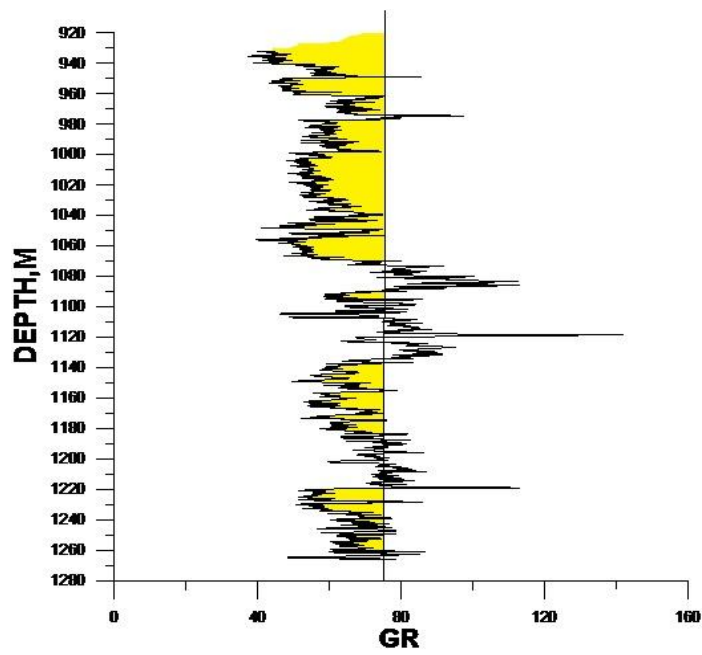


Figure 4: Gama Ray For Well 3

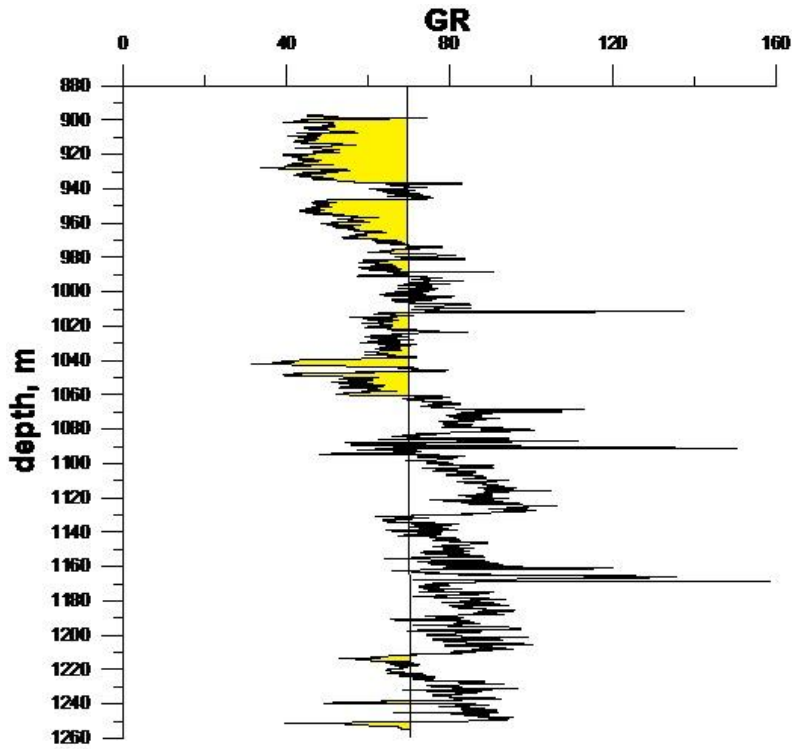


Figure 5: Gama Ray For Well 4

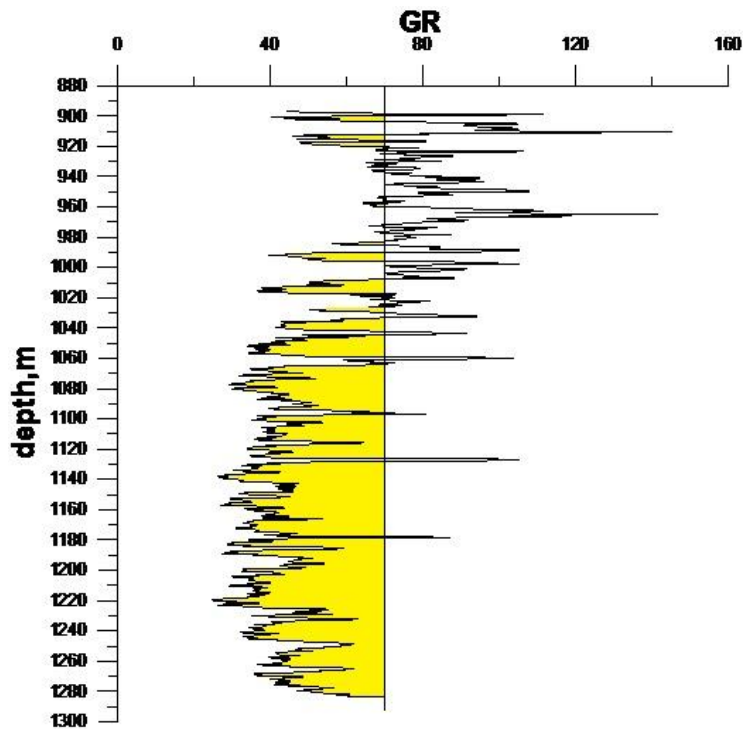


Figure 6: Gama Ray For Well 6

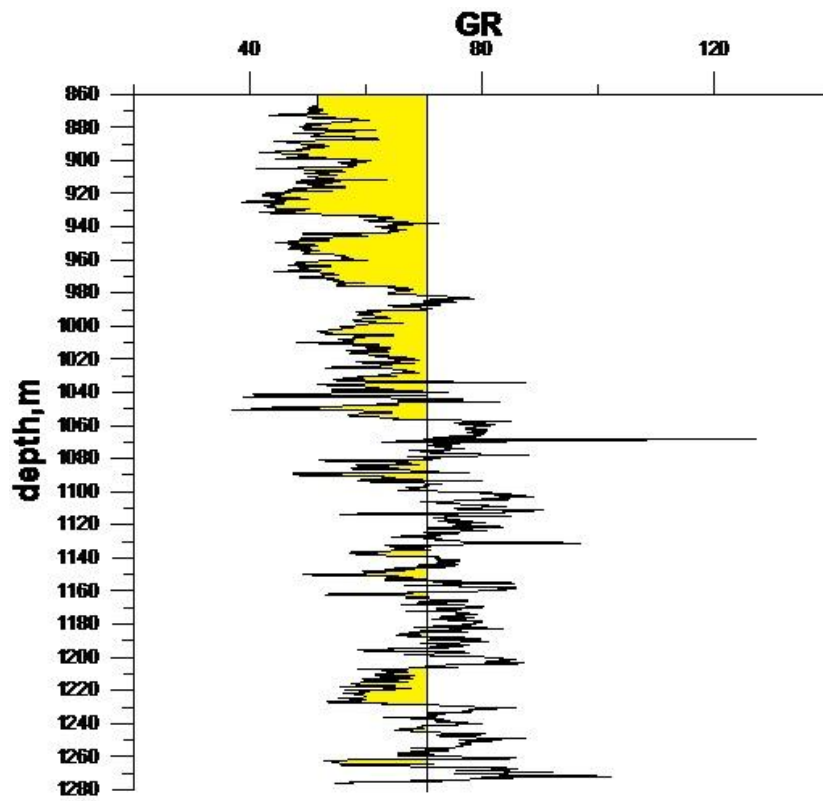


Figure 7: Gama Ray For Well 7

CHAPTER 1..... III

1.1. INTRODUCTION:	خطأ! الإشارة المرجعية غير معرفة.
1.2. GENERAL GEOLOGY:	خطأ! الإشارة المرجعية غير معرفة.
1.3. MUGLAD REGIONAL GEOLOGY:.....	خطأ! الإشارة المرجعية غير معرفة.
1.4. SUDAN GEOLOGICAL:	- 3 -
1.4.1. <i>Muglad Basin</i> :	خطأ! الإشارة المرجعية غير معرفة.
1.4.2. <i>Muglad Basin Stratigraphy</i> :	- 6 -
1.4.3. <i>Greater Bamboo</i>	- 9 -
1.4.4. <i>Structure map and well profile</i> :	- 10 -
1.4.5. <i>Aradeiba Formation</i> :	- 11 -

CHAPTER 2..... - 19 -

2.1. POROSITY	- 20 -
2.1.1. <i>Introduction</i> :	- 20 -
2.1.2. <i>Porosity Types</i> :	- 21 -
2.1.3. <i>The Range of Porosity Values in Nature</i> :	- 22 -
2.1.4. <i>Porosity Logs</i> :.....	- 23 -
2.1.4.1. <i>The Sonic Log</i>	- 23 -
2.1.4.2 <i>The Neutron Log</i>	- 24 -
2.1.4.3 <i>The Density Log</i>	- 24 -
2.1.5. <i>Total Porosity Determination</i> :	- 25 -
2.1.6. <i>Calculating The Porosity</i> :	- 25 -
2.1.7. <i>Porosity by Coring</i> :.....	- 25 -
2.2. PERMEABILITY	- 26 -
2.2.1. <i>Definition and theory</i> :	- 26 -
2.2.2. <i>Controls on Permeability and the Range of Permeability Values</i>	- 28 -
2.2.3. <i>Permeability Determination</i> :	- 29 -
2.2.4. <i>Type of Permeability</i> :	- 29 -
2.2.5. <i>Permeability Relationships</i> :	- 30 -
2.3. POROPerm RELATIONSHIPS.....	- 31 -

CHAPTER 3..... - 34 -

3.1. HYDROSTATIC PRESSURE:	- 35 -
3.2. OVERBURDEN PRESSURE:	- 36 -
3.3. PORE PRESSURE:	- 36 -
3.3.1. <i>Normal Pore Pressure</i> :	- 36 -
3.3.2. <i>Abnormal Pore Pressure</i> :.....	- 37 -

3.3.3. <i>Subnormal Pore Pressure:</i>	- 37 -
3.4. PORE PRESSURE EVALUATION:	- 37 -
3.4.1. <i>Sonic Logs:</i>	- 37 -
3.4.2. <i>Resistivity Logs:</i>	- 39 -
3.4.3. <i>Formation Density Logs:</i>	- 40 -
3.5. SATURATION:	- 40 -
3.5.1. <i>Mathematical expressions for fluid saturation:</i>	- 41 -
3.5.2. <i>Methods to Determination Saturation:</i>	- 42 -
CHAPTER 4.....	- 44 -
4.1. POROSITY CALCULATION	- 44 -
4.1.1. <i>Total porosity:</i>	- 44 -
4.1.2. <i>Effective Porosity:</i>	- 50 -
4.2. PERMEABILITY	- 54 -
4.3. SATURATION:.....	- 58 -
4.4. PORE PRESSURE.....	- 61 -
4.4.1. <i>Numerical Methodology for Pressure Estimation:</i>	- 61 -
4.4.2. <i>Pressure Numerical Estimation:</i>	- 62 -
4.4.3. <i>Pore pressure Estimation Method:</i>	- 62 -
CHAPTER 5.....	- 67 -
RESULT AND DISCUSION	- 67 -
CONCLUSION AND RECOMMENDATION	- 74 -
CONCLUSION :	- 74 -
RECOMMENDATION:	- 75 -
REFERENCES :	- 76 -